Effect of desalination of Sargassum algae on its potential use as a stabilizer in sustainable earth-based bricks

Stanislas Tido Tiwa, Ketty Bilba, Cristel Onésippe Potiron, Marie-Ange Arsene

▶ **To cite this version:**

Stanislas Tido Tiwa, Ketty Bilba, Cristel Onésippe Potiron, Marie-Ange Arsene. Effect of desalination of Sargassum algae on its potential use as a stabilizer in sustainable earth-based bricks. 2024. hal-04697270

HAL Id: hal-04697270
https://hal.science/hal-04697270v1

Preprint submitted on 13 Sep 2024

HAL is a multi-disciplinary open access archive for the deposit and dissemination of scientific research documents, whether they are published or not. The documents may come from teaching and research institutions in France or abroad, or from public or private research centers.

L'archive ouverte pluridisciplinaire **HAL**, est destinée au dépôt et à la diffusion de documents scientifiques de niveau recherche, publiés ou non, émanant des établissements d'enseignement et de recherche français ou étrangers, des laboratoires publics ou privés.

Effect of desalination of *Sargassum* algae on its potential use as a stabilizer in sustainable earth-based bricks

Tido Tiwa Stanislas [1,2], Ketty Bilba [1], Cristel Onésippe Potiron [1], Marie-Ange Arsène [1]

[1] *Université des Antilles, Laboratoire COVACHIM-M2E UR4_2, UFR SEN, Campus de Fouillole, BP 250, 97157 Pointe-à-Pitre, Guadeloupe, France*
[2] *LEME, UPL, Université Paris Nanterre, 50 rue de Sevres, 92410, Ville d'Avray, France*

1- Tido Tiwa Stanislas, Ph.D, Université Paris Nanterre, France, stidotiwa@aust.edu.ng

3- Ketty Bilba, Ph.D, Université des Antilles, Guadeloupe, France, ketty.bilba@univ-antilles.fr

4- Cristel Onésippe Potiron, Ph.D, Université des Antilles, Guadeloupe, France, cristel.onesippe@univ-antilles.fr

5- Marie-Ange Arsène, PhD, Université des Antilles, Guadeloupe, France, Marie-Ange.Arsene@univ-antilles.fr

[*]Corresponding author: E-mail address: stidotiwa@aust.edu.ng (ID: 0000-0002-6726-1112)

Abstract:

Since 2011, Caribbean beaches have been flooded by massive quantities of pelagic *Sargassum*, causing environmental, health and financial problems. The use of *Sargassum* ash as a stabilizer in the manufacture of bricks can help mitigate the economic impact of *Sargassum* grounding by adding value. This study assesses the effect of the Pelagic *Sargassum* algae desalination process on the properties of the biomass as well as the potential application of their ash as a stabilizer in soil-based bricks. Fresh *Sargassum* algae was subjected to two cycles of immersion in water, then calcined under different conditions (temperature and time) and characterized. The desalinated *Sargassum* ash (SA) was used to partially replace cement in the stabilization of earth bricks. Characterization of raw and desalted *Sargassum* shows a reduction in ash content from 28.44 to 17.25% after desalination. Furthermore, the thermo gravimetric analysis show a slight reduction in the initial degradation temperature between 204 and 602 °C, which is associated with a reduction in the amount of residual char from 35% to 27%. The results of the XRF analysis of the SA showed a very low alumiosilica content (SiO_3+Al_2O_3< 4%), but a significant increase in CaO content after desalination from 21.96 to 50.17%. The XRD results of the SA are consistent with the XRF analysis which reveals that the desalination process significantly increased the $CaCO_3$ content from 19 to 67%, while KCl decreased significantly from 26 to 8%. Furthermore, the characterization of the composites reveal that partial substitution of 10 wt.% cement by SA calcined at 700 °C for 2 hours has no significant effect on water absorption, density,

compressive strength and chemical composition of earth bricks. This material could help reduce pollution linked to the decomposition of sargassum on Caribbean coasts and beaches, as well as greenhouse gas emissions linked to cement production.

Keywords: pelagic *Sargassum* algae, *Sargassum* ash, desalination, chemical and mineral composition, earth-based brick

1. Introduction

The massive invasion and proliferation of *Sargassum* algae on Caribbean beaches and coasts in recent years is endangering people's livelihoods, climate-sensitive areas and local ecosystems [1]. This *Sargassum* outbreak problem has prompted several Caribbean countries to declare a national state of emergency [2]. Due to the severe environmental, health and economic impacts associated with the presence, mechanical cleaning and storage of *Sargassum* on coasts and beaches [1], the Caribbean Regional Fisheries Facility has estimated the cost of *Sargassum* clean-up in 2018 at US$210 million [3]. *Sargassum* has traditionally been collected from beaches and coasts for animal feed and fertilizer [1]. But to date, the sheer volume of this algae is challenging researchers to find new applications for this available material [4]. Research to develop sustainable value chains for *Sargassum* to promote economic opportunities that could help mitigate the impacts of mass influxes seems commendable. Although these algae represent a harmful marine resource for many Caribbean countries, they also represent a high-potential energy and building material opportunity that has been little explored.

Several studies have been developed on the valorization of *Sargassum* biomass in the fields of bioremediation, agriculture, biofuels, health, and food [4]–[8]. For example, Paraguay-Delgado et al. [9] analysed each part (vesicles, thallus and leaves) of the *Sargassum* algae and found that the thermal behaviour and ash content were very similar for these three parts of the alga, while the calcite content of the vesicles was relatively low compared to the leaves and thallus. Ávalos-Betancourt et al. [6] evaluated the energy potential of pelagic *Sargassum* spp. algae as solid biofuel using sustainable indicators along the Caribbean Mexican coast from 2015 to 2020. The theoretical estimate demonstrated the possibility of satisfying the annual bioenergy needs for residential heating of 79,163 inhabitants in the said region with the removal of *Sargassum* for only one month along the 600 km coast. This high ash content and the high energy potential of the pelagic biomass of *Sargassum* indicate that it is possible to

use this biomass as a by-product for energy production and to use its ash as a cement substitute for soil stabilization.

Earth materials have been traditionally used in construction since Antiquity [10] due to the various characteristics they possess, such as durability under compressive load [11], low thermal conductivity [12], [13], low energy requirements during manufacturing. More, they do not generate greenhouse gas emissions during their production or lifetime, and are easy to access [14], etc. Therefore, earth-based materials are emerging as an alternative solution to the sustainability problem caused by the extensive use of cement in conventional construction, which results in CO_2 emissions and destabilization of the ecosystem [15]. In addition, over the past decades, researchers have sought to develop "green" alternatives in the construction industry. However, most of the "green" alternatives [16] do not possess the properties required for their use in the construction sector. Therefore, during their processing, certain additives [17], adjuvants [18], etc. are introduced to improve their performance. Agro-industrial by-products or wastes [19], [20] are the most favoured additives as their disposal is very difficult to manage and economically inefficient. Therefore, their use in construction may add value to the waste, reduce its management cost, decrease environmental pollution and contribute to the local economy by creating jobs [21]. Furthermore, the use of waste in construction will contribute to Sustainable Development Goal 11 (SDG11) in the United Nations (UN) Sustainable Development Goals (SDGs) for 2030.

Various stabilizers such as cement [22], lime [23], ash [24], etc. have been widely used to improve the strength and the durability of soil-based materials. Soils are classified as lateritics soils if they have a ratio of silica to sesquioxide [$SiO_2/(Fe_2O_3 + Al_2O_3)$] between 1.33 and 2.00 [24]. However, the effectiveness of using ash from various agricultural wastes as a stabilizer [25]–[27] for lateritic soils has recently been established by several researchers, as it offers environmental, economic and technological advantages over conventional mortars [28]. For example, Obianyo et al. [24] demonstrated that the inclusion of 2 wt.% bone ash and 2 wt. % palm ash significantly improved the compressive strength of lateritic bricks by up to 129% compared to unstabilized bricks after 28 days. This is attributed to pozzolanic reactions between lateritic soil and soil stabilizers (bone ash and oil palm ash) resulting in the formation of cementitious materials (calcium silicate hydrate and calcium aluminate hydrate), which explains the hardening and strengthening of stabilised bricks. In addition, Souza et al. [26] showed that replacing cement with 10 wt.% wood ash improved the compressive strength of mud bricks by 20 % and reduced water absorption by 3%. Assiamah et al. [29] have shown

that replacing ordinary Portland cement with 20 wt.% sawdust ash does no significantly improves the desired technical properties compressive strength and density compared to stabilizer made of 100 wt.% cement for earth bricks. Recently, Nadia et al. [30] evaluated the impact of the recovery of two biomass (WBAa, WBAb; WBA is for Wood Bottom Ash) ashes from domestic wood heating on the thermal, mechanical and durability properties of compressed earth bricks. The results show that the mechanical strength increases with the wood ash content and the curing time. The lowest thermal conductivity properties are obtained with BWBAa, while BWBAb (B is for bricks) shows the best levels of flexural and compressive strength, resulting in the formation of compounds with bonding properties due to its high MgO content. To the authors' knowledge, the use of *Sargassum* seaweed ash as a stabilizer in earth materials has not yet been studied.

This preliminary study attempted to assess the effect of the Pelagic *Sargassum* algae desalination process on the physical, chemical and thermal properties of the biomass as well as the potential application of their ash as a stabilizer in soil-based bricks. The main objective was to investigate the suitability of ash from *Sargassum* algae biomass as a stabilizer for laterite soil bricks. In particular, this work (i) evaluates the effect of desalination of *Sargassum* algae on its thermal degradation, density, porosity and proximate composition, including moisture content, ash content, volatiles and fixed carbon; (ii) assesses the effect of temperature and heating time on the chemical and mineral properties of *Sargassum* ash; and (iii) assesses the effect of substitution of ordinary Portland cement on the compressive strength, density and water absorption of earth-based bricks. This industrial use of *Sargassum* may help reduce the financial cost of cleaning up the coast.

2. Materials and methods

2.1. Raw materials collection and desalination pre-treatment of algae

The *Sargassum* algae used in this study was mainly pelagic *Sargassum* species, consisting of 67 wt.% *Sargassum* fluitans and 33 wt.% *Sargassum* natans algae, collected along the coastline of Grande-Terre, Guadeloupe, from June to July 2022. The fresh *Sargassum* algae were collected in sea water about two metres from the shore to avoid contact of the *Sargassum* algae with the sand. The *Sargassum* was immediately placed in the garbage bag and transported to Université des Antilles for manual sorting and washing with tap water. The algae were rinsed with tap water while the impurities were removed manually before being

divided into two groups: (1) the first group was placed on the pallet for air drying while the second group (2) was subjected to two rounds of tap water immersion for 40 min at a *Sargassum*/water volume ratio of 1:30 [31]. During the desalination of the *Sargassum* algae, the ionic conductivity of the tap water before and after the immersion of the *Sargassum* algae at t =5 min and t = 40 min was determined with conductimeter XS COND 51 PLUS in order to monitor the transfer of salt from the *Sargassum* algae to the fresh water. After desalination, the resulting algae were air-dried for approximately one week to remove as much water as possible. During the drying process, the *Sargassum* algae were turned over once or twice a day to speed up the drying process.

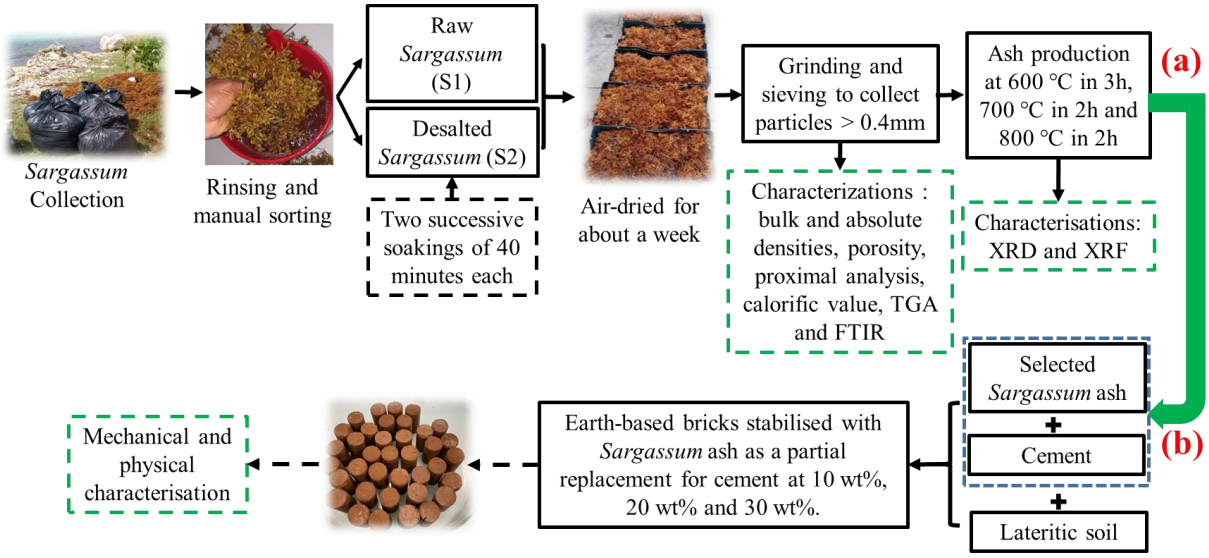

Fig. 1a shows the flow chart for the preparation and characterization of pelagic *Sargassum* algae.

The air dried *Sargassum* algae were crushed and then sieved using a mechanical sieve at 230 rpm for 10 minutes to remove the sand and salt particle lower than 0.4 mm [32].

Fig. 1: Flow chart of (a) the *Sargassum* calcination process and (b) the production of soil bricks stabilised with *Sargassum* ash

2.2. Characterization of raw and desalinated *Sargassum* and earth-based bricks

2.2.1. Proximate analysis: assessment of some physical properties of *Sargassum* algae heating value

The proximate analysis (moisture content, ash content, volatile matter and fixed carbon content) allows the estimation of the physical properties of a biomass that have a direct

influence on its combustion performance [33]. The moisture content of biomass samples was measured by a direct method of weight loss in drying oven according to CEN/TS 14774-1:2009 described by Gravalos et al. [34]. The *Sargassum* algae sample was oven dried for 24 hours at (105 ± 2) °C to a constant mass and the percentage of moisture was calculated from the water loss of the sample according to equation (1).

$$\%\ Moisture\ content = \frac{W_i - W_{od}}{W_{od}} \times 100 \qquad (1)$$

where W_i and W_{od} represent the specimen initial weight and oven-dried weight respectively.

Ash is the inorganic solid residue left after the complete burning of biomass [35]. Approximately 10g of *Sargassum* biomass was subjected to calcination in the muffle furnace at about 550 °C for 2h [36] and the ash content was determined following the equation (2).

$$\%\ Ash = \frac{W_b - W_c}{W_{od}} \times 100 \qquad (2)$$

where W_b: weight of the crucible and ash, W_c: weight of empty crucible and W_{od}: oven-dried weight of the *Sargassum* algae.

Meynell method was used to determine the volatile content (% Volatile) of *Sargassum* biomass according to the methodology described by Achebe et al. [35]. The oven-dried *Sargassum* seaweed was preheated to 250 °C in an oven for 2 hours under air to remove volatile matter. The sample was then heated to 470 °C for 2 hours, just before the material turned black. The volatile matter was determined according to the equation (3).

$$\%\ Volatile = \frac{W_{rd} - W_{ds}}{W_{od}} \times 100 \qquad (3)$$

where W_{rd}: weight sample after heating at 250 °C, W_{ds}: dry sample after heating at 470 °C and W_{od}: oven-dried weight of the *Sargassum* algae.

The fixed carbon content (% FC) of the *Sargassum* biomass was deduced from equation 4, which represents the solid carbon of the biomass remaining after the de-volatilization processes.

$$\%FC = 100\% - (\%\ MC + \%AC + \%VM) \qquad (4)$$

where MC: moisture content, AC: ash content and VM: volatile matter content (% Volatile)

2.2.2. Determination of the density and porosity of *Sargassum* biomass

The samples bulk density (BD) was evaluated according to PN-EN 15103:2010 and described by Mierzwa-Hersztek et al. [37]: the biomass was filled in a calibrated vessel with constant

volume and weighed; the bulk density BD was then calculated as the mass of the sample divided by the vessel volume. A helium pycnometry apparatus (Thermo Electron Corporation) was used to determine the *Sargassum* algae absolute density (ρ_{abs}) according to the procedure described by Mierzwa-Hersztek et al. [37]. The porosity (φ) of the sample was calculated from the bulk density and the absolute density according to equation 5. The experimental was repeated three times.

$$\varphi = \left(1 - \frac{BD}{\rho_{Abs}}\right) \times 100 \qquad (5)$$

where φ is the porosity (%), BD is the bulk density (g/cm^3) and ρ_{abs} the absolute density (g/cm^3).

2.2.3. Fourier Transformed Infrared and Thermo gravimetric analysis of *Sargassum* biomass

The chemical functional groups of desalinated pre-treated and untreated *Sargassum* algae were assessed with Fourier Transform Infrared (FTIR) analysis at the spectra range of 400-4000 cm^{-1} using PerkinElmer UATR Two equipment [38].

Thermogravimetric analysis was also performed on desalinated pre-treated and untreated *Sargassum* algae to evaluate the influence of the desalination pre-treatment on the thermal degradation behavior of the marine biomass. The samples were heated from 40 to 900 °C (10 °C/min) under nitrogen gas flow, using the PerkinElmer precisely STA 6000 [13]. Prior to each measurement, samples were dried at 105 °C for 24 hours.

2.3. Production and characterization of ash

Dried raw (S1) and desalinated *Sargassum* (S2) biomass were subjected to different calcination conditions (Fig. 1) to assess the effect of heating time and temperature on the chemical and mineral compositions of the ash for potential application as a construction material. Approximately 10 g of oven-dried, pre-treated and raw *Sargassum* algae particles larger than 0.4 mm were introduced into a ceramic crucible and transferred to the muffle furnace. In order to optimize the calcination of Sargassum algae, and based on the previous study by Bilba et al. [31] , Sargassum biomass was calcined at 600°C for 2h, 600°C for 3h, 700°C for 2h and 800°C for 2h. However, the ash calcined at 600°C for 2h was not visually completely calcined, so ash calcined at 600°C for 3h, 700°C for 2h and 800°C for 2h was adopted for analysis. Each calcination condition was repeated three times on the same

feedstock (raw S1 and desalinated S2 algae particles) to determine the mean value and standard deviation of ash production yield.

The chemical compositions of *Sargassum* ashes were carried out using the Thermo Scientific X-ray Fluorescence (XRF) Epsilon spectrometer realized at National Geosciences Research Laboratories (NGRL) in Kaduna, Nigeria. While the mineralogical compositions were determined by X-ray diffraction (XRD) using the Rigaku Miniflex 600 diffractometer, model RU 200B (Rigaku Corporation, Japan) with a scan interval of 2Θ from 10 to 70°, an acquisition speed of 2°/min and Cu Kα radiation, in NGRL also [39], [40].

Raw and desalinated *Sargassum* particles and also their corresponding ashes morphology were characterized qualitatively using an Environmental FEI Quanta 250 scanning electron Microscope (ESEM). The micrographs were obtained using Scanning Electron Microscopy with a 15 kV electron acceleration voltage at the center for characterization of the Université des Antilles (Centre Commun de Caractérisation des Matériaux des Antilles et de la Guyane C3MAG, Guadeloupe). This ESEM was equipped with an energy dispersive X-ray spectrometer (EDS) to analyse in several points of the sample surface the semi-quantitative chemical composition of the materials.

2.4. Lateritic soil and cement

Lateritic soil was collected at Sainte-Rose section Bis, Guadeloupe, GPS (lat =16.2791420°, long = -61.6962600°) at a depth of about 2 m. The soil was then dried at 105 °C for 24 hours, crushed and sieved to 400 µm and their plasticity limit was 38% (ASTM D 4318, [41]). Ordinary Portland cement CEM I 42.5 R was used as a stabilizer for the production of earth-based bricks.

2.5. Earth-based bricks: preparation and characterization

The earth-based bricks samples were prepared by mixing lateritic soil with cement in a 90:10 weight ratio (soil:cement) as a reference based on previous studies performed by Stanislas et al. [11]. The cement content was then partially replaced (0%, 10%, 20% and 30% by weight) by desalinated *Sargassum* ash (SA) obtained after calcination at 600 °C and 700 °C (Table 1). The dry solid mixture was obtained by manual agitation of the powdered components for 5 minutes before the gradual introduction of 38% by weight of water corresponding to the

plasticity limit of the soil. The paste was mixed for 5 minutes and transferred to a cylindrical mould with a diameter of 25 mm and a length of 50 mm. The bricks were immediately sealed in the plastic bag and stored in the laboratory for 2 days, then transferred to the curing chamber at a temperature of 60 °C and a relative humidity of 100%. To determine the strength development as well as the physical properties of the manufactured bricks, the specimens were tested after 28 days. The specimens were subjected to a compression test using a Shimadzu universal testing machine under a 10 kN load cell at a speed of 1 mm/min, in Université des Antilles (Groupe de surface et interfaces (GTSI) laboratory). The water absorption, bulk density and apparent void volume of the specimens were determined according to the procedures specified in ASTM C 948 [42], while the specific density was obtained using a helium pycnometer apparatus (Thermo Electron Corporation).

Table 1: Composition of earth-based materials stabilized with cement and *Sargassum* ash

Specimen name	Temperature of ash calcination (°C)	Cement content (wt.%)	Ash content (wt.%)	Lateritic soil content (wt.%)
C10LS90 (Ref.)		10	0	90
600C9SA1LS90	600	9	1	90
600C8SA2LS90	600	8	2	90
600C7SA3LS90	600	7	3	90
700C9SA1LS90	700	9	1	90
700C8SA2LS90	700	8	2	90
700C7SA3LS90	700	7	3	90

Ref.: Reference; C: Cement; SA: *Sargassum* ash; LS: Lateritic soil

MINITAB Release 16 statistics were used to compare the means of each test condition by Turkey's Honestly Significant Difference (HSD) method and examination of variance (ANOVA), one way at the 0.05 significance level.

3. Results and discussion

3.1. Effect of *Sargassum* algae pre-treatment on biomass and ash properties

3.1.1. Ionic conductivity of the soaking solution

Fig. 2 shows the monitoring of tap water conductivity before and during *Sargassum* soaking. The results show that the ionic conductivity of the tap water increases with the immersion time of the *Sargassum* algae, from 79.44 µS/cm to 182.80 µS/cm in only 40 min. This is related to the transfer of salts and other ionic hydrosoluble organic compounds from the biomass to the water [43]. However, the value of ionic conductivity decreases significantly during the second cycle of *Sargassum* algae immersion, with a slight increase from 95.56

µS/cm to 107.24 µS/cm between 5 min and 40 min, value which is closer to tap water conductivity than after only one immersion.

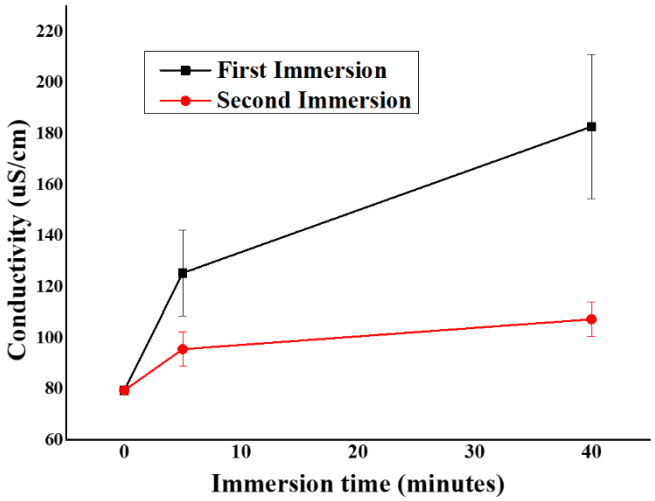

Fig. 2: Evolution of ionic conductivity of tap water after introduction of collected *Sargassum* algae

3.1.2. Proximate analysis of treated and untreated *Sargassum* algae

It is well known [44] that burning fuels with a high moisture content increases the volume of exhaust gases and therefore lowers the combustion temperature. Table 2 shows that there is no significant difference in moisture content for untreated and treated *Sargassum* algae. On the other hand, the volatile matter content increases slightly from 43.74% to 50.82%, the fixed carbon content from 3.29% to 8.37%, while the ash content decreases from 28.44% to 17.25% after desalination. This can be attributed to the desalination process that occurs during the immersion of the *Sargassum* algae, which helps to reduce the amount of non-combustible compounds probably such as KCl, which presence will be confirmed lately by X-ray diffraction. Other studies on algae biomass have shown similar results (Table 2). The present study shows a relatively high moisture content (about 25%) compared to previous results reported in the literature (Table 2). This can be attributed to the fact that the pelagic *Sargassum* was only air-dried. Compared to other non-marine biomass feedstocks, ash contents were significantly higher than those found in terrestrial plants, which rarely exceed 12% by weight [9]. In addition, there is no significant change in volatile matter content as the pre-treatment does not degrade the main *Sargassum* biomass compounds: hemicellulose (devolatilization and carbonization limit below 250 °C), cellulose (decomposition between 305-375 °C) and lignin (decomposition range 250-500 °C) [45].

Table 2. Summary of proximate analysis results for the present work on *Sargassum* biomass and previous studies

Seaweed species	Collection site	Proximate analysis (wt. %)				Reference
		MC	VC	AC	FC	
Sargassum natans (untreated)	China	10.46	48.85	29.09	11.60	[46]
Sacharina japonica (untreated)	Sub Korea	6.90	68.79	20.21	4.1	[47]
Pelagic *Sargassum* (washing)	Mexican Caribbean coast	20	84.59	21.64	-	[6]
Pelagic *Sargassum* (untreated)	Beaches in Mexico	-	-	23.00	-	[9]
Enteromopha clathrata (untreated)	China	10.13	57.99	21.15	10.13	[46]
Pelagic *Sargassum* (untreated)	Beaches in Guadeloupe	24.53 ± 0.09	43.74 ± 1.48	28.44 ± 0.36	3.29 ± 1.16	Present study
Pelagic *Sargassum* (desalinated)	Beaches in Guadeloupe	23.59 ± 0.33	50.82 ± 0.33	17.25 ± 0.61	8.37 ± 0.52	

*MC: Moisture content; AC: Ash content; VM: Volatile matter; FC: Fixed Carbon content

3.1.3. Bulk density, absolute density, porosity and fuel value index of *Sargassum* biomass

Table 3 presents the bulk and absolute densities and porosity of raw and desalinated *Sargassum* algae. The results show a slight reduction in density from 0.193 g/cm^3 to 0.171 g/cm^3 and in absolute density from 1.249 g/cm^3 to 1.241 g/cm^3 of the *Sargassum* algae after desalination, while there is a slight increase in its porosity from 84.59% to 86.18%. This can be attributed to the removal of salt particles deposited on the surface of the *Sargassum* algae during immersion. In addition, the slight increase in the porosity of the *Sargassum* biomass due to the desalination pre-treatment can be related to the presence of new pores formed during the process, which affects the volume of the material. In contrast, Freitas et al. [48] subjected dealginated residue of *Sargassum filipendura* algae to an acidic pre-treatment process to reduce their silver content. The results reveal an increase in bulk density from 0.881 to 0.932 g/cm^3 and absolute density from 1.472 to 1.552 g/cm^3 after the pre-treatment. According to the authors, this slight increase in density, which results in a slight reduction in porosity from 40.15% to 39.95% of the dealginated residue, is attributed to the fact that silver ions have no influence on the filling of empty pores. Compared to the results of Freitas et al. [48] (Table 3), the density obtained in the present study is relatively low, while the porosity is

high. This difference may be related to the specie and to the dealgination process applied to the *Sargassum filipendura* algae. However, the density and porosity of raw and desalinated *Sargassum* biomass are similar to some plant biomasses, including wheat straw, miscanthus straw and sawdust [37] which are regularly used as solid biofuel.

Table 3: Mean values and standard deviation of densities and porosity of *Sargassum* biomass and some other plant biomasses

Sargassum samples	Bulk density (g/cm^3)	Absolute density (g/cm^3)	Porosity (%)	Reference
Raw pelagic *Sargassum* algae (S1)	0.193 ± 0.008	1.249 ± 0.001	84.59	Present study
Desalinated pelagic *Sargassum* algae (S2)	0.171 ± 0.006	1.241 ± 0.001	86.18	
Dealginated residue of *Sargassum filipendura* algae	0.881	1.472	40.15	[48]
Acid pre-treated of dealginated residue of *Sargassum filipendura* algae	0.932	1.552	39.95	
Wheat straw	0.143 ± 0.013	1.464 ± 0.314	90.3	[37]
Miscanthus straw	0.152 ± 0.015	1.430 ± 0.152	89.4	
Bark	0.460 ± 0.021	1.766 ± 0.561	73.9	
Sawdust	0.313 ± 0.072	1.502 ± 0.235	79.2	

3.1.4. FTIR analysis of *Sargassum* algae

FTIR spectra in Fig. 3 present the functional group of *Sargassum* seaweed before and after treatment. The peak at 580 cm^{-1} is typical band representing Si-O-Si possibly from quartz due to the presence of sand [24].This peak intensity reduces after the treatment of *Sargassum* algae, which can be due to the partial removal of sand particle during washing process. The bands at 873 cm^{-1} and 1028 cm^{-1} are related to C-O stretching vibration which are derived from polysaccharide of *Sargassum* [49]. These peak absorbances slightly decrease with the desalination process. The peak at wave number 1235 cm^{-1} in the treated and untreated *Sargassum* is associated to the C-O-C stretching vibration of the aryl-alkyl ether compound in the cellulose [38]. The bands at 1423 cm^{-1} and 1622 cm^{-1} indicate the symmetric and anti-symmetric stretches of carboxylate groups, respectively. The band with the wave number of 1622 cm^{-1} is also attributed to the vibration of primary amides in amino acids, but the band is mainly attributed to alginate carboxylate [50]. The absorption peak at 1927 cm^{-1} indicates the C-H stretching vibration of the methyl and methylene groups, which is attributed to the presence of lignin [49]. In addition, at 3277 cm^{-1}, the broader peak is typical band representing O-H stretching vibration of the carboxylic, phenolic and alcoholic groups, which

is attributed to polysaccharides in *Sargassum* biomass [10], [38]. However, with the exception of the decrease of some peaks observed on *Sargassum* at wavenumbers 580cm^{-1}, 873cm^{-1}, 1423cm^{-1} and 2927cm^{-1}, after desalination, no functional group disappeared due to the pre-treatment.

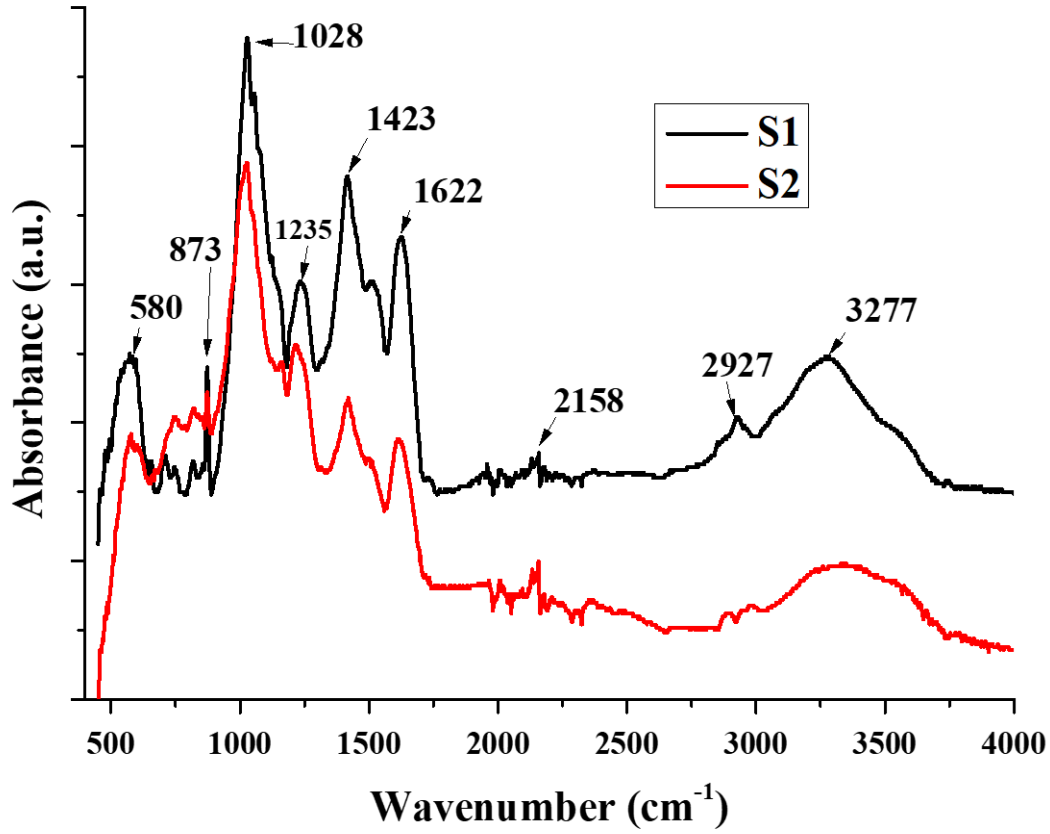

Fig. 3: Infrared spectra of untreated (S1) and desalinated pretreated (S2) *Sargassum* biomass

3.1.5. Thermo gravimetric analysis of *Sargassum* algae

Fig. 4 shows the thermogravimetric or mass loss with temperature (TGA, Fig. 4a) and derivative analysis of mass loss (DTG, Fig. 4b) curves of pelagic *Sargassum* algae before (S1) and after desalination pre-treatment (S2). The results reveal that TGA curves (Fig. 4a) are constituted of three zones in correlation to the pyrolysis results of various marine seaweed materials [7], [9], [51], [52]. Zone I shows a very low percentage of mass loss (≈17% for S1 and ≈20% for S2) due to dehydration in the temperature range of 40 to 204 °C because of the removal of water from pelagic *Sargassum* algae. The degradation of zone II occurs between 204 and 602 °C and displays the highest mass degradation (≈35% for S1 and ≈41% for S2), which is related to the removal of various amounts of biopolymers from the algae [7], [53]. The complex chemical reactions promoted by decarbonization and degradation of important

structural polymers, such as hemicellulose, cellulose and lignin, occur in this zone [54]. The final degradation above 602 °C (zone III) is attributed to the combustion of carbonaceous residues triggered by intense heating [55]. The residual char, left at 900 °C, after the calcination of untreated and treated *Sargassum* are 35% and 27% respectively. This reduction of the residual char content of desalinated *Sargassum* can be attributed to its low salt content compared to untreated algae (see Section 3.1.6.) [56]. In addition, this amount of residual charcoal is significantly high compared to the fixed carbon (FC) value estimated at 3.3 wt.% for S1 and 8.4 wt.% for S2, which may indicate the presence of organic compounds (cellulose, hemicellulose and lignin)) in the *Sargassum* algae. Fig. 4b of DTG curve shows that the first degradation after dehydration of untreated and treated *Sargassum* algae starts at 204 °C with the peak at 267 °C, 337 °C and 425 °C for untreated *Sargassum* and 258 °C, 339 °C and 425 °C for the pre-treated *Sargassum* algae [13], [57]. This degradation temperature of *Sargassum* biomass suggests their potential to be used as reinforcement ageing in inorganic matrix such as cement and organic matrix such as polymer composite without affecting their structural integrity during mixing, curing and densification process at a temperature below 204 °C.

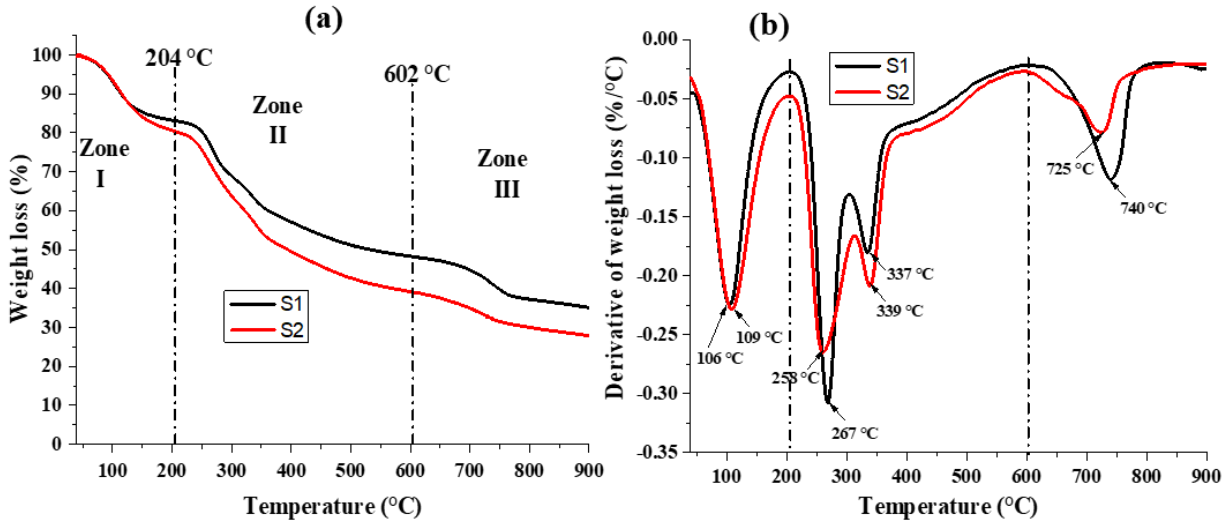

Fig. 4: (a) Mass loss during heating (TGA) and (b) derivative of the mass loss during heating (DTG) of *Sargassum* seaweed before (S1) and after desalination pre-treatment (S2)

3.1.6. Chemical composition of *Sargassum* ash

According to Gonzalez-Lopez et al. [58] and Li et al. [59] the chemical and mineralogical composition of the biomass significantly influences the ash production temperature. Fig. 5

reported the ash contents (Fig. 5a) and chemical composition of *Sargassum* ash (Fig. 5b, c) produced from raw and desalinated *Sargassum* algae.

Fig. 5a shows that the ash content decreases with increasing calcination temperature by about 13.6% for S1 and 20.5% for S2 at a temperature between 550 °C and 800 °C. This can be due to the fact that calcination of the *Sargassum* algae at a temperature below 700 °C was not sufficient to degradate all the inorganic compounds present in the *Sargassum* biomass [58]. Ash with a homogeneous colour was obtained after 2h calcination of raw *Sargassum* algae at 800 °C, while calcination at 600 °C for 3h was sufficient to degrade desalinated *Sargassum*. Furthermore, compared to raw *Sargassum* algae, desalinated *Sargassum* algae has a low ash content (Fig. 5a), which can be attributed to the partial removal of salt, inorganic compounds and/or hydrosoluble compounds in the *Sargassum* biomass during the desalination process. In addition, this may be due to the fact that the removal of harmful compounds such as Cl and K salts in biomass requires a heating temperature above 1200 °C [58].

Fig. 5b reveals significantly low amounts (< 5 wt.%) of alumina (Al_2O_3) and silica (SiO_2) compounds as for untreated and desalinated *Sargassum* algae after calcination. In addition, for these ashes, the sum of (SiO_2 + Al_2O_3 + Fe_2O_3) is 4.329%. This shows that *Sargassum* ash cannot be used as a pozzolanic material according to ASTM C618 [60] which classifies pozzolanic materials as materials with a sum of SiO_2, Al_2O_3 and Fe_2O_3 at least equal to 70 wt.%. On the other hand, the ash showed a significant increase in CaO content after desalination up to 15% while the chlorine (Cl) content decreased significantly from 21.76% to 5.95% after the calcination of the desalinated material. A similar trend is observed for K_2O which decreases from 26.12% to 13.63% after the desalination process (Fig 5b). After calcination of the desalinated *Sargassum* biomass at 700 °C for 2h, the CaO content move from 34.93% to 50.17%. This high amount of CaO and the low amount of Cl and K_2O in *Sargassum* ash after the desalination process suggest its potential application as a partial replacement for cement materials in the stabilization of earth-based materials in order to promote sustainable construction and reduce environmental concerns related to cement production and *Sargassum* disposal [24], [28], [61].

Furthermore, Figure 5b shows that, for the soil, the sum (SiO_2 + Al_2O_3 + Fe_2O_3) is 80.7% (greater than 70%), so according to ASTM C618 [60], this soil can be classified as pozzolanic material. The ratio of silica to sesquioxide [SiO_2/(Fe_2O_3 + Al_2O_3)] is 0.8 (less than 1.33), which classifies the soil as laterite [24]. In addition, Fig. 5c shows that the main cations in raw and desalinated *Sargassum* ashes are K, Ca and Mg, while Cl and S are the most common

anions. However, this study shows that the amount of Cl in raw *Sargassum* ash is more than 19% while it is less than 6% in desalinated *Sargassum* ash. Similar results were reported by Haykiri-Acma et al. [62] on the ash of two species of brown algae where only the chlorine content reached 12.27%. The potassium content dominates the composition of ash produced from raw *Sargassum* algae at 600 °C for 2 hours, which would pose serious problems for the potential use of this biomass in combustion or gasification [62]. In general, the results show that exposure of raw and desalinated *Sargassum* biomass to different calcination temperatures results in thermal decomposition of their organic and inorganic compounds, giving different colours to the ash depending on the chemical composition of the algae precursor. Calcination of desalinated *Sargassum* at 700 °C for 2 hours is considered to be the most appropriate temperature to generate ash, which can be used to replace cement in building materials due to its high CaO content estimated at 50.17wt.%. Indeed in the presence of water (H_2O), CaO forms $Ca(OH)_2$, which reacts with silica (SiO_2) and aluminate (Al_2O_3) in the soil to form new materials such as calcium silicate hydrates (CSH or $(CaO)_x(SiO_4)_y(H_2O)_z$), and calcium aluminate hydrates (CAH, $(CaO)_x(Al_2O_3)_y(H_2O)_z$), which are mainly responsible for the strength of the materials [63].

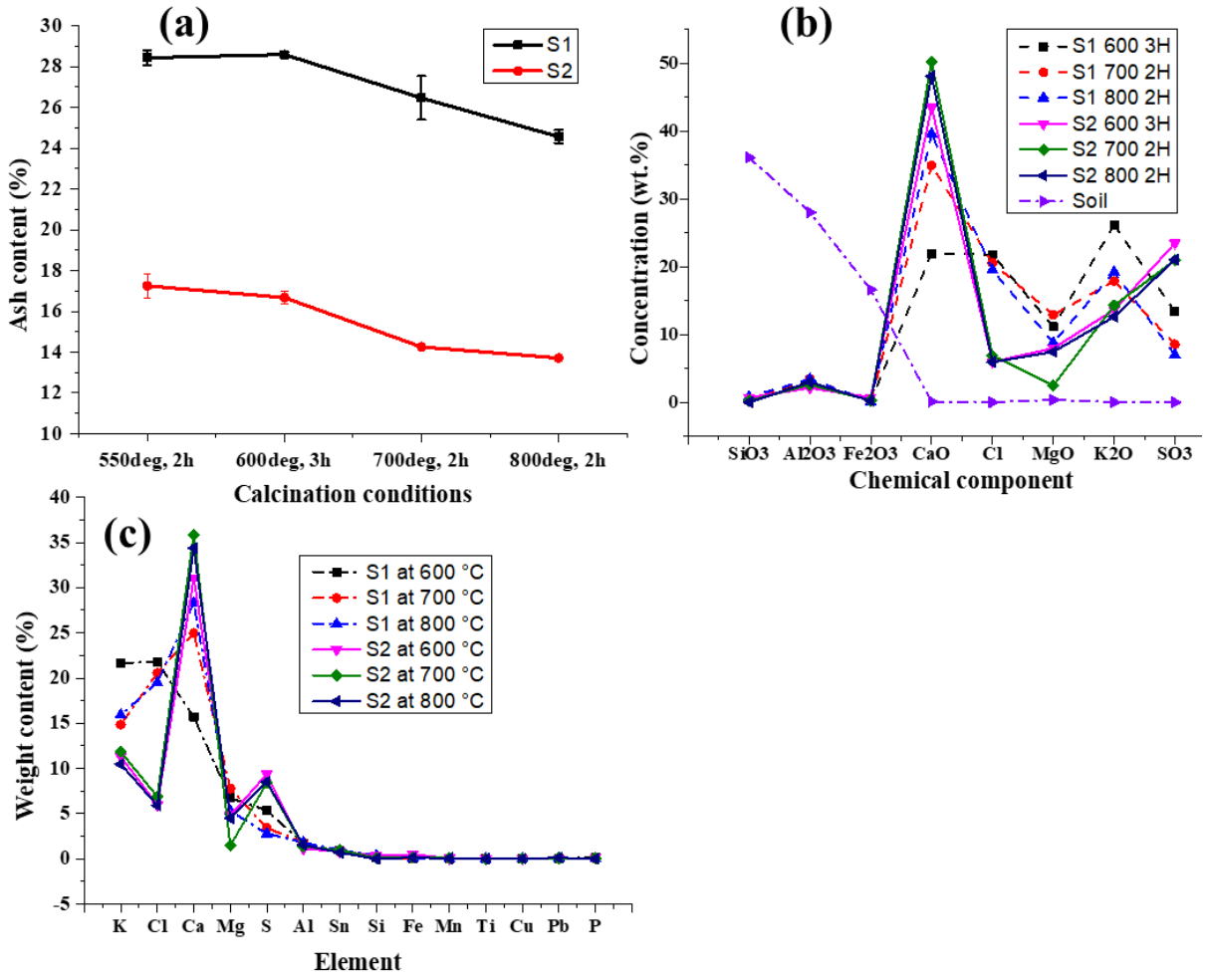

Fig. 5: (a) Ash content of untreated (S1) and desalinated (S2) *Sargassum* after various calcination conditions; (b) oxide contents of *Sargassum* algae ash and (c) elemental composition of untreated (S1) and desalinated (S2) *Sargassum* ash

3.1.7. X-ray diffraction analysis of untreated and treated *Sargassum* ash produced in various conditions

Fig. 6 shows XRD patterns of raw (S1) and desalinated (S2) *Sargassum* pelagic ash, while Table 4 shows the main mineral contents of these ashes produced between 600 and 800 °C. The results show that at 600 °C, S1 ash is mainly composed of chlorapatite (C_h), sylvite (S) and calcite (C), while S2 ash is mainly composed of calcite (C). The untreated ash sample has a $CaCO_3$ content of 19-33 wt.%, and increasing with temperature in the range 600-800 °C, which is relatively low compared to the desalinated ash estimated to decrease with temperature from 67 to 32 wt.% in the same temperature range. However, the KCl content of the untreated and desalinated ash is of the same order of magnitude, ranging from 26-30 wt.%

and 8-25 wt.% respectively. This predominance of the mineral phases calcite, sylvite and chlorapatite in ashes of samples S1 and S2 confirms the abundance of the elements Ca, K, Cl found by XRF analysis (Fig. 5). In addition, the high $CaCO_3$ content in desalinated *Sargassum* algae ash is consistent with chemical analysis which reported an increase in CaO in ash after the desalination pre-treatment of the *Sargassum* algae, resulting in the decreasing, of KCl mineral. The calcite ($CaCO_3$) and alkali chloride contents of ash from raw *Sargassum* fell within the results reported by [36] estimated at (17.99- 42.07%) for calcite and 23.93% for sylvite in pelagic *Sargassum* algae. Furthermore, according to Haykiri-Acma et al., [62] the high concentration of sylvite (KCl) mineral in the ash can be related to the high chlorine content of the algae.

However, Table 4 shows that at a calcination temperature of 800 °C, no difference can be found between the mineral composition of S1 and S2 *Sargassum* ash.

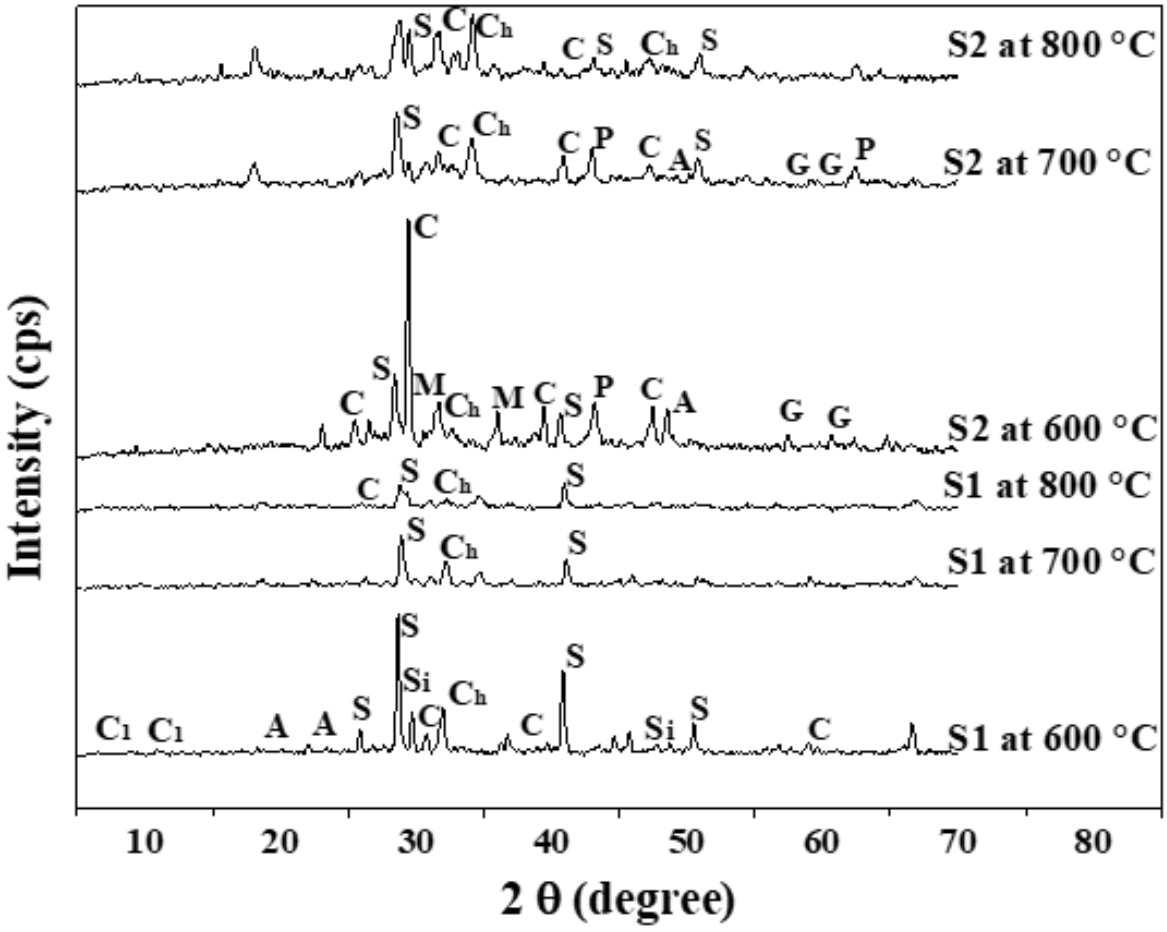

Fig. 6: XRD patterns of *Sargassum* ash obtained from raw (S1) and desalinated (S2) biomass at different temperatures. A: Anhydrite ($CaSO_4$); C: Calcite ($CaCO_3$); C_h: Chlorapatite ($Ca_5Cl(PO_4)$; C_1: Chlorite ($(Mg,Fe)_5(Al,Si)_5\ O_{10}\ (OH)_4$); G: Garnet (3(Ca, Fe, Mg)O.(Al, Fe,

SiO_4); M: Marialite ($Na_4Al_3Si_9O_{24}Cl$); P: Periclase (MgO); S: Sylvite (KCl); Si: Silvialite ($Ca_4Al_6(SiO_4)_6SO_4$).

Table 4: Mineral composition of *Sargassum* ash at different calcination conditions

Ash samples	Ash from raw *Sargassum* (S1)			Ash from desalinated *Sargassum* (S2)		
Temperature (°C)/Time	600 °C/3h	700 °C/2h	800 °C/2h	600 °C/3h	700 °C/2h	800 °C/2h
Calcite ($CaCO_3$)	19 %	31%	33%	67%	45%	32%
Sylvite (KCl)	26%	27%	30%	8%	10%	25%
Chlorapatite ($Ca_5Cl(PO_4)$)	37%	31%	25%	7%	26%	39%
Silvialite ($Ca_4Al_6(SiO_4)_6SO_4$)	14%	4%	3%	-	-	-
Anhydrite ($CaSO_4$)	1.4%	2%	4%	10%	1.9%	1%
Chlorite $(Mg,Fe)_5(Al,Si)_5\ O_{10}\ (OH)_4$	2%	4%	5%	-	-	-
Marialite ($Na_4Al_3Si_9O_{24}Cl$)	-	-	-	7%	-	-
Periclase (MgO)	-	-	-	11%	-	-
Garnet (3(Ca, Fe, Mg)O.(Al, Fe, SiO_4)	-	-	-	1%	2.9%	3%

Table 4 shows that the heating temperature affects the factor of desalination (ratio between the initial mass of the chlorinated solid and its remaining mass after desalination). Working on the relative proportions and considering (1) that the rinsing desalination does not affect the calcite content (whose solubility is much lower than that of KCl and chlorapatite) and (2) that only the compounds containing Cl pass partly in solution, the comparison between S1 and S2 calcinated at 600 °C/3h for example (Table 5) shows that :

- A $CaCO_3$/Cl ratio equal to 67/(8+7+7) is obtained for S2. This ratio is equal to 19/x for S1, where x is the pourcentage of Cl remaining after the rinsing of S1. According to this equality (67/22 = 19/x), x can be calculated as x=19*22/67= 6.2%.
- Using this calculation, the evolution of the calcite composition can be explained by the initial content of chlorides, which decreases from 63% (26+37) to 6.2% or by a factor of desalination equal to 10.
- A similar calculation can be made at 700 °C and 800 °C, and it is proposed in Table 5. The effect of desalination on the Cl content is especially important when the calcination temperature of the ash is low and this effect is no longer sensitive at 800 °C.

Table 5: Summary of the desalination factor for Sargassum algae

Calcinated Temperature (°C)	Amount of compounds containing Cl in S1 ash (%)	Amount of compounds containing Cl remaining in S1 ash after rinsing (%)	Desalination factor
600	63.0	6.2	≈10
700	58.0	24,8	≈2
800	55.0	66.0	≈1

1

2 **3.2.Effect of partial substitution of cement by *Sargassum* ash on earth-based bricks**
3 **properties**

4 **3.2.1. Microstructural analysis (SEM/EDX) of feedstock, ash and earth-based bricks**

5 Fig. 7 presents the micrographs of *Sargassum* biomasses (Fig. 7a and b) and *Sargassum* ashes
6 (Fig. 7c and d). From Fig. 7a and b, it is visible that pelagic *Sargassum* seaweed is constitute
7 by stem, float and leaf with allow them to float on the surface of the sea water. In addition, no
8 significant modification of the surface and morphology were found between raw (Fig. 7a) and
9 desalinated *Sargassum* ashes (Fig. 7c). Furthermore, the morphological aspect of raw (Fig.
10 7c) and desalinated (Fig. 7d) *Sargassum* ash reveal homogeneous particles with irregular
11 shapes which confer a rough surface aspect. Similar observation was highlighted by Souza et
12 al. [26].

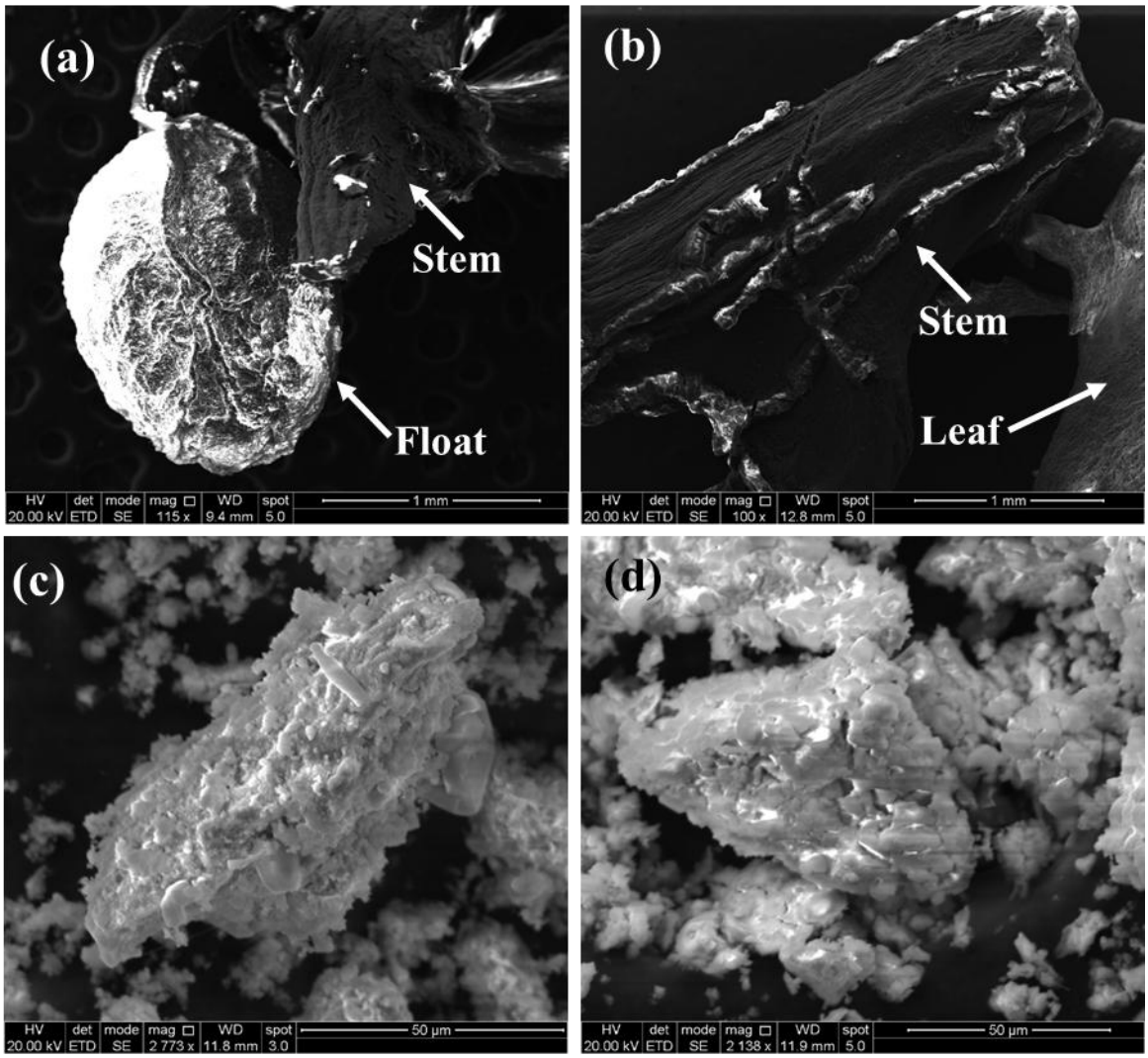

Fig. 7: SEM micrographs of (a) raw *Sargassum* and (b) desalinated *Sargassum,* and ashes calcinated from desalinated *Sargassum* (c) at 600 °C (SA600) and (d) at 700 °C (SA700)

Figure 8 illustrates the microscopic morphology of the reference brick (Figure 8a) and the brick resulting from the substitution of cement with 30% by weight of desalinated *Sargassum* ash at 600 °C (SA600) and at 700 °C (SA700), at 28 days. The morphology of 600C7SA3LS90 (Fig. 8b) revealed a coarse agglomerated flake appearance with an alveolar and granular surface, with some porosity caused by the wide particle size distribution of the mixture. This may be also attributed to the incomplete pozzolanic reaction of the material [30]. However, Fig. 8c shows that the morphology of 700C7SA3LS90 is dominated by dense material with a alveolar and spherical structure. The products take the form of blocks forming a dense, compact brick as the pozzolanic reaction takes place. The atomic concentrations presented in high content in C10LS90 (Reference) were O, Si, Al, Fe and Ca estimated at 71.14%, 11.64%, 9.56%, 4.27% and 3.38% respectively, and the main proportions presented

in 600C7SA3LS90 and 700C7SA3LS90 were the same compared to C10LS90 with different proportions: 71.38%, 10.69%, 9.01%, 5.13% and 3.79% respectively for 600C7SA3LS90 and, 73.82%, 10.94%, 9.03%, 3.05% and 2.71% respectively, for 700C7SA3LS90. In addition, 700C7SA3LS90 bricks show the highest amount of O element and the presence of another component such as Mg (0.45%), which is consistent with the XRF result of the ash. Similar atoms were observed by Nadia et al. 2023 [30] on soil bricks stabilised with wood ash. According to the authors, the presence of O, Si, Al, Ca and Mg reflects the presence of the cementitious products CSH (Calcium Silicate Hydrates), CAH (Calcium Aluminate Hydrates) and MSH (Magnesium Silicate Hydrates) in the material.

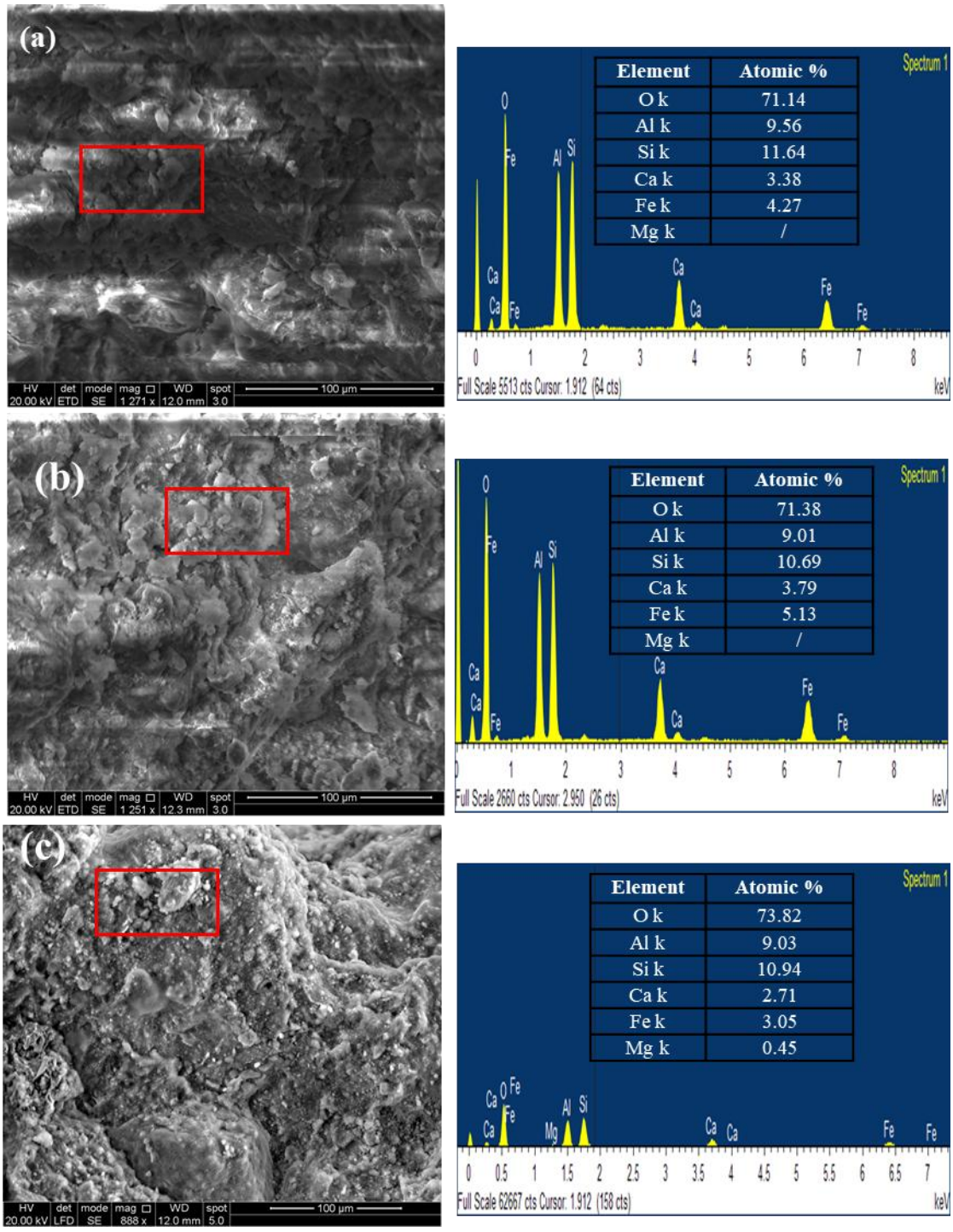

Fig. 8: SEM micrographs and EDX analysis of (a) reference brick (C10LS90), (b) 600C7SA3LS90 and (c) 700C9SA1LS90 after 28 days, where aCxSAyLSz (a: ash production temperature, C: cement, x: cement content by weight, SA: *Sargassum* algae ash, y: ash content by weight, LS: soil, z: soil content by weight)

3.2.2. FTIR Analysis of the earth based bricks

Fig. 9 shows the spectra of earth bricks stabilized with cement and *Sargassum* ash calcined at 700°C for 2 hours. The results show that the spectra are dominated by Si-O-Si stretching, Si-O bending, Si-O-Al bending and O-H stretching bands. In bricks stabilized only with cement (C10LS90) and stabilized with cement and *Sargassum* ash, these bands are present with a slight reduction in intensity for 700C9SA1LS90 and 700C7SA3LS90. This can be attributed to the substitution of Si-O bonds by Si-O-Al, leading to the dissolution of reactive phases (silicon, aluminium) [14].

While the SEM-EDX results indicate the presence of O, Si, Al, Ca, Fe and Mg (Fig. 8), Table 6 reveals the predominance of the silicate (Si-O and Si-O-Si) and aluminosilicate (Si-O-Al) functional group in the bricks. In addition, the O-H stretching and bending vibration peaks show the chemical bonding of water in the soil stabilised with cement and *Sargassum* ash. The hydration reaction generates calcium hydroxide from calcium oxide, which reacts with carbon dioxide in the air. However, the carbonation reaction increases the bonding between soil particles [23], leading to an increase in compressive strength due to the formation of C-S-H (hydrated calcium silicate).

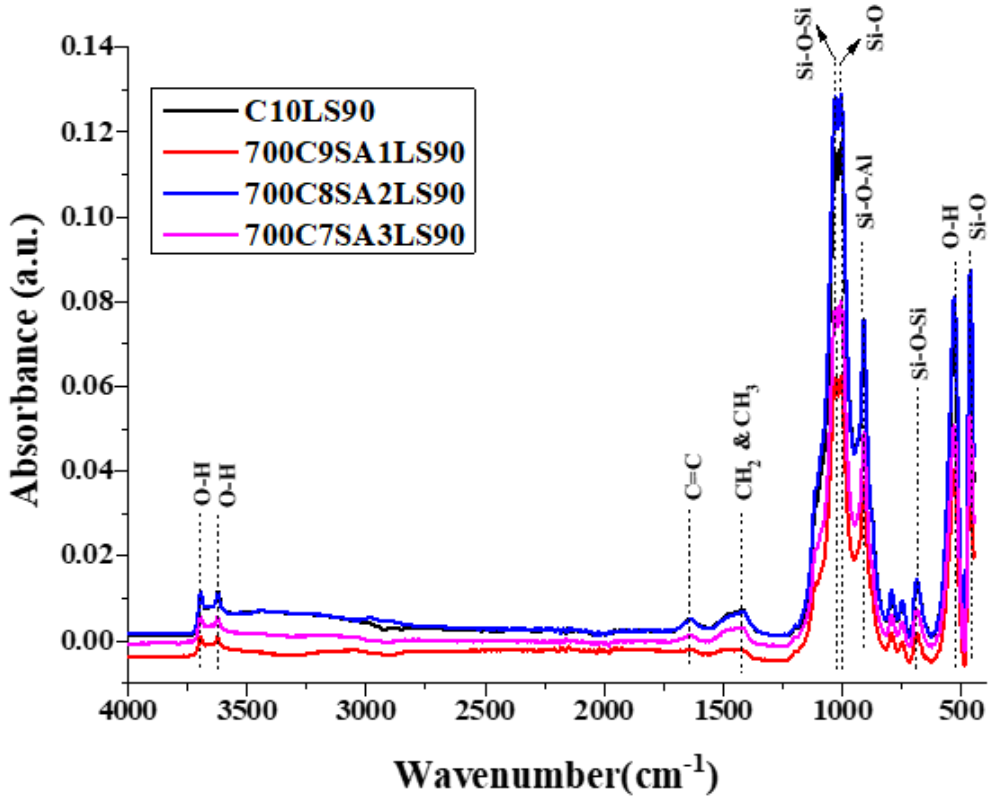

Fig. 9: Infrared spectra of earth-based bricks stabilised with 10% of cement (C10LS90) and the substitution of cement with *Sargassum* ash calcinated at 700 °C at 1, 2 and 3 wt.%.

Table 6: Peaks and functional groups present in the various earth-based bricks

C10LS90 (cm^{-1})	700C9SA1LS90 (cm^{-1})	700C8SA2LS90 (cm^{-1})	700C7SA3LS90 (cm^{-1})	Functional Group
3695, 3622	3695, 3622	3695, 3622	3695, 3622	O-H stretching
1645	1645	1645	1645	C=C stretching
1429	1433	1429	1433	CH_2 & CH_3 bending
1003	1004	1004	1004	Si-O bending
910	910	910	910	Si-O-Al bending
687	687	688	688	Si-O-Si stretching
534	534	534	534	O-H bending
465	465	465	465	Si-O bending

700: Temperature in degree Celsius; C: Cement; SA: *Sargassum* ash; LS: Lateritic soil

3.2.3. Physical properties of the earth based materials

Fig. 10 present the bulk density (10a), specific density (10b) and water absorption (10c) of earth-based bricks at 28 days. The bulk density results reveal that earth bricks produced with ash calcined at 600 °C and 700 °C show similar trends at 28 days. For bricks produced with *Sargassum* ash calcined at 600 °C from S2, the bulk density of the composite decreases when cement is replaced by *Sargassum* ash. Furthermore, the decreasing of the bulk density is significant only for bricks containing 3wt.% of *Sargassum* ash calcined at 700 °C. For both calcination temperatures, based on the mean value and standard deviation, there is no significant difference between the bulk density of the bricks when the cement is replaced by 1 and 3 wt.% of *Sargassum* ash. However, the results of the specific density presented on the curves in Fig. 9b show the same trend, passing through a minimum at 2% by weight of ash, whatever the calcination temperature. A crossover in the density trend curves for bricks incorporating ash calcined at 600 and 700 °C is observed at around 2.7 wt.%.

For water absorption by bricks (Fig. 10c), it can be seen that at 28 days of hardening, the water absorption of bricks stabilised with cement and *Sargassum* algae ash increases regularly as the ash content calcined at 700 °C is added, whereas the addition of 1% by weight of SA calcined at 600 °C leads also to an increase in water absorption before reducing slightly to 2 wt.% ash. This is due to the rough surface of the two ashes, which results in high water retention in the composition and a high number of voids [26]. The significantly high water absorption of bricks stabilised with 9 wt.% of cement and 1 wt.% of *Sargassum* ash calcined at 600°C for 3 hours (Fig. 10c) can be attributed to their high porosity (Fig. 10d). Previous research [26], [30] show that the water absorption of earth bricks increases progressively with the substitution of cement in the composite. However, the sudden increase in water absorption

in this sample when cement is replaced at 1% by weight can be attributed to the presence of defects in the materials, which increase their density and porosity.

Fig. 10d shows the relationship between porosity determined from equation 5, water absorption and the percentage of desalinated *Sargassum* algae ash calcined at 600 °C for 2h in earth bricks. The results reveal that the introduction of the ash content in the earth-based brick increases the porosity and the water absorption of the brick. In addition, porosity and water absorption show the same trend, indicating the ability of water to fill voids. The porosity is between 56 and 58%, which means that half of the material is made up of voids. This value results in low packing density and poor contact between particles [64]. This could be attributed to the production method, which can negatively affect the mechanical performance and positively affect the thermal insulation properties of clay bricks [65].

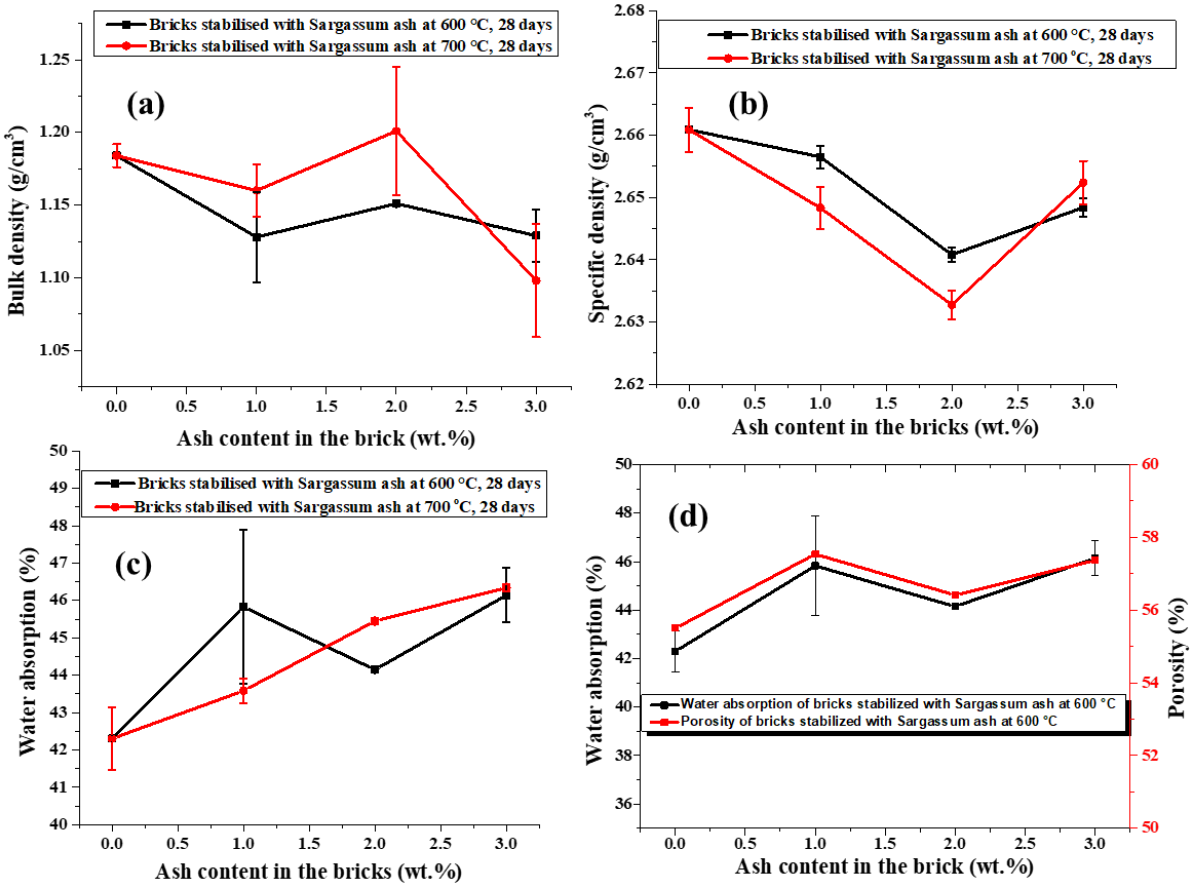

Fig. 10: Effect of desalinated *Sargassum* algae ash inclusion on (a) bulk density, (b) specific density and (c) water absorption of stabilized lateritic earth bricks, and (d) relationship between porosity, water absorption and desalinated *Sargassum* algae ash content in the earth-based brick.

3.2.4. Compressive strength of earth-based materials

Table 7 shows the mean compressive strength and modulus of elasticity (Young's modulus) of earth-based materials stabilised with desalinated *Sargassum* algae calcined at 600 °C and desalinated *Sargassum* algae calcined at 700 °C as partial replacement of cement at 10 wt.%, 20 wt.% and 30 wt.% after 28 days of hardening and Fig. 11 shows the corresponding graphs. Overall, the results show that the compressive strength of bricks containing desalinated *Sargassum* algae calcinated at 600 °C range from 1.29-4.19 MPa, while the bricks of desalinated *Sargassum* algae calcinated at 700 °C range from 2.12-6.21 MPa. After 28 days of curing, the binder incorporating desalinated algae ash calcined at 700 °C has the highest compressive strength. These results are consistent with the chemical composition of desalinated *Sargassum* algae calcined at 700 °C, which shows higher levels of calcium oxide (Fig. 5b) and magnesium oxide. In the presence of water, a pozzolanic reaction occurs between the CaO in the *Sargassum* ash and (SiO_2 and Al_2O_3) in the lateritic soil, forming hydrated products with binding properties. According to Eliche-Quesada et al. [66], these products are similar to those formed during the hydration of Portland cement in this case (C-S-H, C-A-H and/or C-A-S-H). Furthermore, additional C-S-H gel can be formed during the faster hydration of the cement due to the pozzolanic reaction with the ash, which reinforces the rigidity of the matrix [67]. The mechanical properties are therefore in line with the expected pozzolanic reactions. In addition, with the exception of the 600C9SA3LS90 formulation made with partial replacement of the cement by 30% by weight of desalinated *Sargassum* algae calcined at 600 °C, the compressive strength of the bricks obtained is greater than 2 MPa, which is the minimum value required by French standard XP P13-901 [68] for earth wall building materials. Furthermore, the compressive strength value of these earth-based bricks can be compared with results found in the literature. For example, Assiamah et al. [29] used sawdust burnt ash as a partial replacement for cement in interlocking blocks at 10, 20 and 30 wt.% and the compressive strength ranged from 4.73 to 6.52 MPa which are of the same order of magnitude as C10LS90. However, Souza et al [26] used wood ash as a partial substitute for cement at 0, 10, 20 and 30 wt.% in the manufacture of earth-based bricks and the results showed that the compressive strength was between 1.15 and 2.24 MPa, generally lower than that of the study.

It should be noted that pozzolanic reactions could be more numerous in earth bricks stabilised with cement and desalinated *Sargassum* algae calcined at 700 °C, because the mineralogical composition of this ash is richer in calcium oxide (CaO) (Fig. 5b). Silica and alumina

recombine with calcium to form complex calcium aluminate hydrates (C-A-H) and calcium silicate hydrates (C-S-H) [63], which act as binders and help to improve the mechanical properties and durability of materials.

After 28 days of hardening, the modulus of elasticity of bricks stabilized with cement and desalinated *Sargassum* algae calcined at 600 °C decreases as the cement is replaced by desalinated *Sargassum* algae at 30% by weight. However, for the modulus of elasticity of bricks stabilized with cement and desalinated *Sargassum* algae calcined at 700 °C, there is no real trend. So, to obtain bricks with a high Young's modulus, it would be better to work at 700 °C to calcine algae, since this calcination temperature does not degrade the modulus of elasticity. These results are linked to the high calcium and magnesium oxide contents. In the presence of water, MgO reacts with silica to produce magnesium-silicates-hydrates (M-S-H) which take part to enhance mechanical performance of the material [30]. In addition, several authors demonstrated that from the point of view of the pozzolanic reaction products of MgO and SiO_2 are similar to those of CaO. For example, Espuelas et al. [69] reported that MgO is considered an alternative binder for the manufacture of earth-based bricks and leads to the development of compressive strength better than CaO.

Table 7: Compressive performances of lateritic soil bricks stabilised with cement and desalinated *Sargassum* algae at 28 days, expressed as mean ± standard deviation

Specimen	Compressive strength (MPa)	Modulus of elasticity (MPa)
C10LS90	5.59 ± 1.40a	203.56 ± 27.41abcd
600C9SA1LS90	2.84 ± 0.76bcde	232.92 ± 47.56abcd
700C9SA1LS90	5.06 ± 1.15ab	375.15 ± 71.54a
600C8SA2LS90	3.31 ± 0.85abcde	223.50 ± 26.18abcd
700C8SA2LS90	4.05 ± 0.48abcd	263.50 ± 40.17abc
600C7SA3LS90	1.47 ± 0.18de	119.08 ± 24.01cd
700C7SA3LS90	2.50 ± 0.38cde	247.04 ± 67.08abc

*Value with distinct letters in the same column signify statistical difference resulted from Tukey post-hoc test ($p < 0.05$).

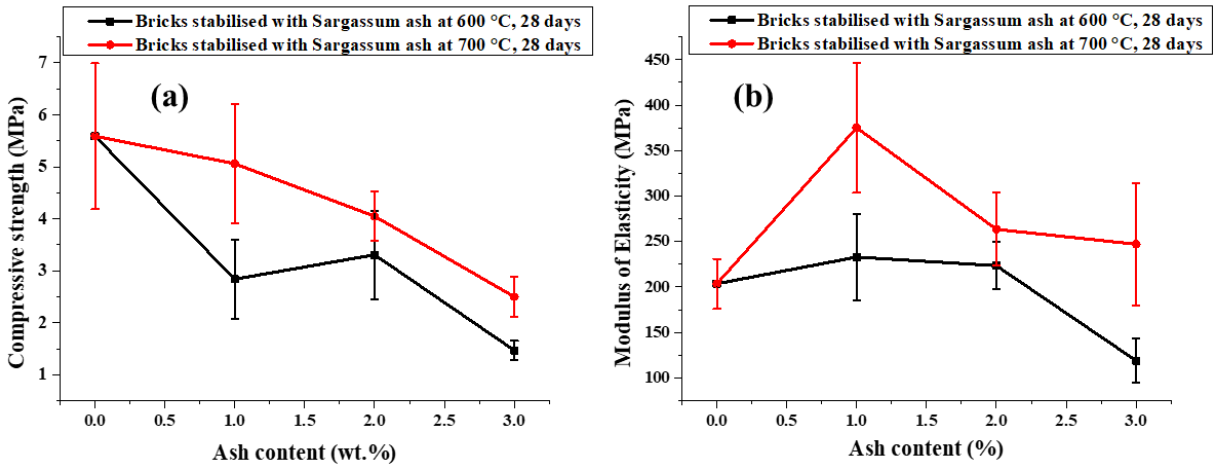

Fig. 11: Effect of ash inclusion obtained from desalinated *Sargassum* on (a) compressive strength and (b) modulus of elasticity of lateritic earth bricks stabilized with cement and *Sargassum* ash at 28 days.

3.2.5. Cross-analysis of results and choice of soil binder stabilized with cement and desalinated *Sargassum* algae ash

In order to select the optimum binder formulation, the physico-chemical and mechanical characteristics at 28 days of the binders produced are compared (Table 8), and technological constraints are also taken into account. In this table, the characteristics of binders stabilized with cement and ash are compared with those of the control binder, which is stabilized with cement only. A plus sign (+) indicates that this property is greater than that of the control binder and a minus sign (-) indicates the opposite, i.e. that the property is less than that of the control binder. The greater the number of (+) or (-) signs, the greater the difference between the control binder and the binder stabilized with cement and desalinated *Sargassum* algae ash is.

Table 8: Cross-analysis of characteristics at 28 days, compared with cement-stabilised binder C10LS90

Stabilised binder	Water absorption	Porosity accessible to water	Specific density	Compressive strength	Young's modulus
C10LS90	Control binder (reference)				
600C9SA1LS90	+++	~	~	-	~
600C8SA2LS90	++	~	--	-	~
600C7SA3LS90	+++	+	--	--	--
700C9SA1LS90	+	~	-	~	+

700C8SA2LS90	++	++	--	~	~
700C7SA3LS90	+++	~	-	--	~

In terms of technological considerations, the binder used to produce the future composites must have mechanical properties at least equal to those of the control binder, while it absorbes less water as possible. From a mechanical point of view, only formulations 700C9SA1LS90 and 700C8SA2LS90 maintain mechanical properties at least equal to those of the control binder. Taking water absorption into account, the binder that absorbs the least amount of water is the 700C9SA1LS90 formulation. Consequently, according to the cross-analysis of the results and the technological criteria, the optimum binder formulation is 700C9SA1LS90, which is the one that can be suitable to make composites. This binder also has the advantage of being lighter than the control binder.

Furthermore, based on the yield of ash production at 700°C for 2h (Fig. 5a), to manufacture 1000 kg of 700C9SA1LS90 containing 1% by weight of sargassum ash (approximately 115 bricks of 315mm×150mm×95mm), the quantity of dry sargassum should be 140 kg (10 kg × 14) and the quantity of fresh sargassum required should be 1540 kg (140 kg × 11). Consequently, the use of *Sargassum* biomass to partially replace cement in the stabilisation of earth bricks may help to alleviate the environmental, financial and health problems associated with the decomposition of Sargassum algae along the beaches and coast of the Caribbean.

In addition, although there is a slight overall reduction in the mechanical performance of the bricks (Fig. 11a and b), the compressive strength of the 700C9SA1LS90 binder exceeds the minimum value of 2 MPa set by French standard XP P 13-901 for cement and ash stabilised earth bricks intended for residential infill walls [68].

4. Conclusion

This study evaluates the effect of the desalination process of pelagic *Sargassum* algae through two cycles of immersion in water on its physico-chemical and thermal decomposition behaviour as well as on the yield of ash production, its chemical and mineral composition. The compressive mechanical behaviour of earth bricks stabilized with cement and desalinated *Sargassum* algae is also studied. According to the results described above, the subsequent conclusions can be expressed:

- Monitoring the ionic conductivity of the tap water during immersion reveals a significant decrease (around 40%) in the ionic conductivity of water from 182.80 µS/cm at the end of the first immersion to 107.24 µS/cm after the second immersion of *Sargassum* algae;
- Proximate analysis of the *Sargassum* algae shows a significant reduction in ash content from 28.44% to 17.25% after desalination, while volatile matter and fixed carbon content increased. However, there was a slight reduction in bulk density from 0.192 g/cm^3 to 0.171 g/cm^3 and in absolute density from 1.249 g/cm^3 to 1.241 g/cm^3, while porosity increased from 84.59% to 86.18%;
- The thermogravimetric study of *Sargassum* algae shows that the *Sargassum* desalination process slightly reduces the degradation temperature of the first zone of the *Sargassum* algae from 267 °C to 258 °C, which is associated with a significant reduction in the amount of residual charcoal from 35 wt.% to 27 wt.%;
- Although the chemical composition of the ash showed a very low aluminosilica content (SiO_3+Al_2O_3 < 4%), a significant increase, in CaO content, after desalination up to 15% was observed while K and Cl contents decreased significantly up to 48% for K and 73% for Cl after the desalination process;
- The XRD spectra of *Sargassum* ash are consistent with the XRF analysis which reveals that the desalination process significantly increased the calcite ($CaCO_3$) content from 19% to 67%, while sylvite (KCl) decreased significantly from 26% to 8%;
- The SEM/EDX study of earth-based bricks reveals the predominance of O, Si, Al, Ca and Mg, which reflects the presence of the cementitious products as CSH, CAH and MSH in the material;
- Based on the results obtained in case of earth-bricks for water absorption, density, compressive strength and modulus of elasticity, the 700C9SA1LS90 formulation performed best, that is to say that the properties of the binder stabilised with desalinated *Sargassum* algae and cement are at least equal to the control (C10LS90). These results are consistent with the chemical composition of desalinated *Sargassum* algae calcinated at 700 °C (SA700), which has higher levels of calcium oxide and magnesium oxide.

Chemical and mineral analyses of raw (S1) and desalted (S2) sargassum ash show a significant increase in CaO content and a reduction in KCl after pre-treatment, demonstrating the potential for desalted sargassum ash to be used as a partial substitute for cementitious materials in soil stabilisation to reduce greenhouse gas emissions from cement production.

Declaration of interest

The authors declare that they have no known competing financial interests or personal relationships that could have appeared to influence the work reported in this paper.

Acknowledgments

The authors would like to thank Ebed FLEURIMA, Corine JEAN-MARIUS and Mathieu ADOUE for their help in preparing and characterizing the samples. The authors would also like to thank the National Geosciences Research Laboratories (NGRL) in Kaduna, Nigeria, for their collaboration in the XRD and XRF analyses of the ash. They also would like to thank the Centre Commun de Caractérisation des Matériaux des Antilles et de la Guyane (C^3MAG-Université des Antilles France) and the Engineering Department of UFR Sciences Exactes et Naturelles (Université des Antilles).

Funding statement

The authors gratefully thank the ANR *Sargassum* program "Holistic approach for *Sargassum* valorization - SARGOOD" supported by ANR, FAPESP, INTERREG Caraïbes (Administrative numbers: SARGD01/2020/06/04/06/STC/FDE/H, Synergie numbers: 7266).

References:

[1] I. Tobío-Pérez, A. Alfonso-Cardero, Y. Díaz-Domínguez, S. Pohl, R. Piloto-Rodríguez, and M. Lapuerta, "Thermochemical Conversion of Sargassum for Energy Production: a Comprehensive Review," *Bioenergy Res.*, no. 0123456789, 2022, doi: 10.1007/s12155-021-10382-1.

[2] A. Desrochers, S. A. Cox, H. A. Oxenford, and B. Van Tussenbroek, "Sargassum uses guide: a resource for Caribbean researchers, entrepreneurs and policy makers," *Rep. Funded by Prep. Clim. Chang. Adapt. East. Caribb. Fish. Sect. Proj. Food Agric. Organ.*, p. 172, 2020.

[3] D. Davis *et al.*, "Biomass composition of the golden tide pelagic seaweeds Sargassum fluitans and S. natans (morphotypes I and VIII) to inform valorisation pathways," *Sci. Total Environ.*, vol. 762, p. 143134, 2021, doi: 10.1016/j.scitotenv.2020.143134.

[4] A. M. López-Contreras, M. Van Der Geest, B. Deetman, S. Van Den Burg, and H. Brust, *Opportunities for valorisation of pelagic Sargassum in the Dutch Caribbean*. 2021. [Online]. Available: www.wur.eu/wfbr

[5] H. Rahbari, A. Akram, M. Pazoki, and M. Aghbashlo, “Bio-Oil Production from Sargassum Macroalgae: A Green and Healthy Source of Energy,” *Jundishapur J. Heal. Sci.*, vol. In Press, no. In Press, 2019, doi: 10.5812/jjhs.84301.
[6] C. A. Ávalos-Betancourt, L. B. López-Sosa, M. Morales-Máximo, A. Aguilera-Mandujano, J. C. Corral-Huacuz, and R. E. Rodríguez-Martínez, “Assessment of the energy potential as a solid biofuel of Sargassum spp. considering sustainability indicator,” *IOP Conf. Ser. Earth Environ. Sci.*, vol. 912, no. 1, 2021, doi: 10.1088/1755-1315/912/1/012010.
[7] L. B. López-Sosa *et al.*, “A prospective study of the exploitation of pelagic sargassum spp. As a solid biofuel energy source,” *Appl. Sci.*, vol. 10, no. 23, pp. 1–17, 2020, doi: 10.3390/app10238706.
[8] T. M. Thompson, B. R. Young, and S. Baroutian, “Pelagic Sargassum for energy and fertiliser production in the Caribbean: A case study on Barbados,” *Renew. Sustain. Energy Rev.*, vol. 118, no. November 2019, p. 109564, 2020, doi: 10.1016/j.rser.2019.109564.
[9] F. Paraguay-Delgado, C. Carreño-Gallardo, I. Estrada-Guel, A. Zabala-Arceo, H. A. Martinez-Rodriguez, and D. Lardizábal-Gutierrez, “Pelagic Sargassum spp. capture CO2 and produce calcite,” *Environ. Sci. Pollut. Res.*, vol. 27, no. 20, pp. 25794–25800, 2020, doi: 10.1007/s11356-020-08969-w.
[10] A. Aboubakar *et al.*, “Dimensionnal stability and strength appraisal of termite hill soil stabilisation using hybrid bio-waste and cement for eco-friendly housing,” *Heliyon*, vol. 8, no. May, p. e09406, 2022, doi: 10.1016/j.heliyon.2022.e09406.
[11] T. T. Stanislas *et al.*, “Effect of Cellulose Pulp Fibres on the Physical, Mechanical, and Thermal Performance of Extruded Earth-based Materials,” *J. Build. Eng.*, vol. 39, no. July, p. 102259, 2021.
[12] A. Aboubakar *et al.*, “Assessment of hygrothermal and mechanical performance of alkali activated Borassus fiber reinforced earth-based bio-composite,” *J. Build. Eng.*, vol. 62, no. October, p. 105411, 2022, doi: 10.1016/j.jobe.2022.105411.
[13] T. T. Stanislas *et al.*, “Potential of raffia nanofibrillated cellulose as a reinforcement in extruded earth-based materials,” *Case Stud. Constr. Mater.*, vol. 16, 2022, doi: 10.1016/j.cscm.2022.e00926.
[14] A. A. Mahamat, N. L. Bih, O. Ayeni, P. A. Onwualu, H. Savastano, and W. O. Soboyejo, “Development of sustainable and eco-friendly materials from termite hill soil stabilized with cement for low-cost housing in chad,” *Buildings*, vol. 11, no. 3, pp. 1–16, 2021, doi: 10.3390/buildings11030086.
[15] J. Zhang, G. Liu, B. Chen, D. Song, J. Qi, and X. Liu, “Analysis of CO2 Emission for the cement manufacturing with alternative raw materials: A LCA-based framework,” *Energy Procedia*, vol. 61, pp. 2541–2545, 2014, doi: 10.1016/j.egypro.2014.12.041.
[16] E. B. Ojo *et al.*, “Mechanical performance of fiber-reinforced alkali activated un-calcined earth-based composites,” *Constr. Build. Mater.*, vol. 247, p. 118588, 2020, doi: 10.1016/j.conbuildmat.2020.118588.
[17] T. T. Stanislas *et al.*, “Performance and Durability of Cellulose Pulp-Reinforced Extruded Earth-based Composites,” *Arab. J. Sci. Eng.*, no. 0123456789, 2021, doi: 10.1007/s13369-021-05698-1.
[18] F. Stazi, A. Nacci, F. Tittarelli, E. Pasqualini, and P. Munafò, “An experimental study on earth plasters for earthen building protection: The effects of different admixtures and surface treatments,” *J. Cult. Herit.*, vol. 17, pp. 27–41, 2016, doi: 10.1016/j.culher.2015.07.009.
[19] O. Ayeni *et al.*, “Effect of coir fiber reinforcement on properties of metakaolin-based geopolymer composite,” *Appl. Sci.*, vol. 12, no. 11, p. 5478, 2022.

[20] S. Tido Tiwa, *Earth-based construction materials reinforced with tropical plants and recycled waste cellulose pulp fibre: performance and durability assessment*, no. February. African University of Science and Technology, Abuja, 2021.
[21] X. Chen *et al.*, "Valorization of construction waste materials for pavements of sponge cities: A review," *Constr. Build. Mater.*, vol. 356, no. September, p. 129247, 2022, doi: 10.1016/j.conbuildmat.2022.129247.
[22] T. T. Stanislas *et al.*, "Multivariate regression approaches to predict the flexural performance of cellulose fibre reinforced extruded earth bricks for sustainable buildings," *Clean. Mater.*, vol. 7, no. December 2022, 2023, doi: 10.1016/j.clema.2023.100180.
[23] I. I. Obianyo, A. P. Onwualu, and A. B. O. Soboyejo, "Mechanical behaviour of lateritic soil stabilized with bone ash and hydrated lime for sustainable building applications," *Case Stud. Constr. Mater.*, vol. 12, no. January, p. e00331, 2020, doi: 10.1016/j.cscm.2020.e00331.
[24] I. I. Obianyo *et al.*, "Performance of lateritic soil stabilized with combination of bone and palm bunch ash for sustainable building applications," *Cogent Eng.*, vol. 8, no. 1, p. 1921673, 2021.
[25] D. Gupta and A. Kumar, "Performance evaluation of cement-stabilized pond ash-rice husk ash-clay mixture as a highway construction material," *J. Rock Mech. Geotech. Eng.*, vol. 9, no. 1, pp. 159–169, 2017, doi: 10.1016/j.jrmge.2016.05.010.
[26] P. C. Souza, E. S. S. Nascimento, L. Melo, H. A. Oliveira, V. G. O. Almeida, and F. M. C. Melo, "Study for the incorporation of wood ash in soil-cement brick," *Ceramica*, vol. 68, no. 385, pp. 38–45, 2022, doi: 10.1590/0366-69132022683853052.
[27] N. L. Bih, A. A. Mahamat, C. Chinweze, and O. Ayeni, "The Effect of Bone Ash on the Physio-Chemical and Mechanical Properties of Clay Ceramic Bricks," no. March, 2022, doi: 10.3390/buildings12030336.
[28] R. Paiva, A. Paiva, L. Caldas, and O. A. M. Reales, "Earth-Based Mortars : Mix Design , Mechanical Characterization and Environmental Performance Assessment," no. June, 2021, doi: 10.4028/www.scientific.net/CTA.1.271.
[29] S. Assiamah, S. Agyeman, K. Adinkrah-Appiah, and H. Danso, "Utilization of sawdust ash as cement replacement for landcrete interlocking blocks production and mortarless construction," *Case Stud. Constr. Mater.*, vol. 16, no. February, p. e00945, 2022, doi: 10.1016/j.cscm.2022.e00945.
[30] B. Nadia, K. Fatma, and C. Nasser, "Mechanical, thermal and durability investigation of compressed earth bricks stabilized with wood biomass ash," *Constr. Build. Mater.*, vol. 364, no. June 2022, p. 129874, 2023, doi: 10.1016/j.conbuildmat.2022.129874.
[31] K. Bilba, C. Onésippe Potiron, and M. A. Arsène, "Invasive biomass algae valorization: Assessment of the viability of Sargassum seaweed as pozzolanic material," *J. Environ. Manage.*, vol. 342, no. January, 2023, doi: 10.1016/j.jenvman.2023.118056.
[32] M. Francoeur *et al.*, "Activated carbon synthetized from Sargassum (sp) for adsorption of caffeine: Understanding the adsorption mechanism using molecular modeling," *J. Environ. Chem. Eng.*, vol. 9, no. 1, 2021, doi: 10.1016/j.jece.2020.104795.
[33] C. A. Buckner *et al.*, "Biomass Pretreatment and Characterization: A Review," *Intech*, vol. 11, no. tourism, p. 13, 2016, [Online]. Available: https://www.intechopen.com/books/advanced-biometric-technologies/liveness-detection-in-biometrics
[34] I. Gravalos, P. Xyradakis, D. Kateris, and T. Gialamas, "An Experimental Determination of Gross Calorific Value of Different Agroforestry Species and Bio-Based Industry Residues," pp. 57–68, 2016.

[35] C. Achebe, A. Umeji, and J. Chukwuneke, “Energy Evaluation of Various Compositions of Biomass Waste Briquettes,” *Adv. Res.*, vol. 13, no. 6, pp. 1–11, 2018, doi: 10.9734/air/2018/39270.
[36] J. J. Milledge, S. Maneein, E. Arribas-López, and D. Bartlett, “Sargassum Inundations in Turks and Caicos : Methane,” *Energies*, vol. 13, pp. 1–27, 2020.
[37] M. Mierzwa-Hersztek, K. Gondek, M. Jewiarz, and K. Dziedzic, “Assessment of energy parameters of biomass and biochars, leachability of heavy metals and phytotoxicity of their ashes,” *J. Mater. Cycles Waste Manag.*, vol. 21, pp. 786–800, 2019.
[38] T. T. Stanislas *et al.*, “Production and Characterization of Pulp and Nanofibrillated Cellulose from Selected Tropical Plants,” *J. Nat. Fibers*, vol. 00, no. 00, pp. 1–17, 2020, doi: 10.1080/15440478.2020.1787915.
[39] G. C. Komadja *et al.*, “Geotechnical and geological investigation of slope stability of a section of road cut debris-slopes along NH-7, Uttarakhand, India,” *Results Eng.*, vol. 10, no. May, 2021, doi: 10.1016/j.rineng.2021.100227.
[40] A. D. Nkapleweh, J. F. Tendo, F. B. Ebanda, P. M. A. Noah, A. E. Mewoli, and T. T. Stanislas, “Physico-chemical and mechanical characterization of triumfetta Pentandra bast fiber from the equatorial region of Cameroon as a potential reinforcement of polymer composites,” *J. Nat. Fibers*, vol. 19, no. 16, pp. 13106–13119, 2022.
[41] ASTM, “4318-00,(2003), Standard Test Methods for Liquid Limit, Plastic Limit, and Plasticity Index of Soils,” *Annu. B. ASTM Stand. Am. Soc. Test. Mater. West Conshohocken, PA*, vol. 4, pp. 582–595, 2003.
[42] A. S. M. for T. ASTM, “ASTM C 948-81: Standard Test Method for Dry and Wet Bulk Density, Water Absorption, and Apparent Porosity of Thin Sections of Glass-Fiber Reinforced Concrete,” 2009.
[43] A. M. Zafar, M. A. Javed, and A. Aly Hassan, “Unprecedented biodesalination rates–Shortcomings of electrical conductivity measurements in determining salt removal by algae and cyanobacteria,” *J. Environ. Manage.*, vol. 302, no. PA, p. 113947, 2022, doi: 10.1016/j.jenvman.2021.113947.
[44] T. Vitoussia, “Thermogravimetric analyses and kinetic modeling of pellets built with three Cameroonian biomass,” *Biomass Convers. Biorefinery*, 2019.
[45] T. T. Stanislas *et al.*, “Potential of raffia nanofibrillated cellulose as a reinforcement in extruded earth-based materials,” *Case Stud. Constr. Mater.*, vol. 16, no. November 2021, 2022, doi: 10.1016/j.cscm.2022.e00926.
[46] S. Wang, Q. Wang, X. Jiang, X. Han, and H. Ji, “Compositional analysis of bio-oil derived from pyrolysis of seaweed,” *Energy Convers. Manag.*, vol. 68, pp. 273–280, 2013, doi: 10.1016/j.enconman.2013.01.014.
[47] S. S. Kim, H. V. Ly, G. H. Choi, J. Kim, and H. C. Woo, “Pyrolysis characteristics and kinetics of the alga Saccharina japonica,” *Bioresour. Technol.*, vol. 123, pp. 445–451, 2012, doi: 10.1016/j.biortech.2012.07.097.
[48] G. R. de Freitas, M. G. A. Vieira, and M. G. C. da Silva, “Fixed bed biosorption of silver and investigation of functional groups on acidified biosorbent from algae biomass,” *Environ. Sci. Pollut. Res.*, vol. 26, no. 36, pp. 36354–36366, 2019, doi: 10.1007/s11356-019-06731-5.
[49] X. L. Zhi Wang, Yuechi Che, Jian Li, Wenzhu Wu, Beibei Yan, Yingxiu Zhand, Xutong Wang, Fan Yu, Guanyi Chen, Xiaoyu Zuo, “Effects of anaerobic digestion pretreatment on the pyrolysis of Sargassum: Investigation by TG-FTIR and Py-GC/MS.” Energy Conversion and Management, p. 115934, 2022.
[50] O. G. J. Robson C. Oliveira, Peter Hammer, Eric Guibal, Jean-Marie Taulemesse, “Characterization of Metal Support Interactions in the lanthanum (III) biosorption on

Sargassum sp. using SEM/EDX, FTIR, and XPS: Preliminary studies," no. 239. Chemical Engineering Journal, 2014.
[51] K. Wu *et al.*, "Pyrolysis characteristics and kinetics of aquatic biomass using thermogravimetric analyzer," *Bioresour. Technol.*, vol. 163, pp. 18–25, 2014, doi: 10.1016/j.biortech.2014.03.162.
[52] M. Tukaram Bai and P. Venkateswarlu, "Fixed bed and batch studies on biosorption of lead using Sargassum Tenerrimum powder: Characterization, Kinetics and Thermodynamics," *Mater. Today Proc.*, vol. 5, no. 9, pp. 18024–18037, 2018, doi: 10.1016/j.matpr.2018.06.136.
[53] S. S. Kim, H. V. Ly, J. Kim, J. H. Choi, and H. C. Woo, "Thermogravimetric characteristics and pyrolysis kinetics of Alga Sagarssum sp. biomass," *Bioresour. Technol.*, vol. 139, pp. 242–248, 2013, doi: 10.1016/j.biortech.2013.03.192.
[54] I. Ali and A. Bahadar, "Thermogravimetric characteristics and non-isothermal kinetics of macro-algae with an emphasis on the possible partial gasification at higher temperatures," *Front. Energy Res.*, vol. 7, no. FEB, 2019, doi: 10.3389/fenrg.2019.00007.
[55] Y. Kumar, A. Tarafdar, D. Kumar, K. Verma, M. Aggarwal, and P. C. Badgujar, "Evaluation of Chemical, Functional, Spectral, and Thermal Characteristics of Sargassum wightii and Ulva rigida from Indian Coast," *J. Food Qual.*, vol. 2021, 2021, doi: 10.1155/2021/9133464.
[56] L. M. Díaz-Vázquez, A. Rojas-Pérez, M. Fuentes-Caraballo, I. V. Robles, U. Jena, and K. C. Das, "Demineralization of Sargassum spp. macroalgae biomass: Selective hydrothermal liquefaction process for bio-oil production," *Front. Energy Res.*, vol. 3, no. FEB, pp. 1–11, 2015, doi: 10.3389/fenrg.2015.00006.
[57] M. Kadivar, C. Gauss, T. Tiwa, A. Javad, S. Charca, and H. Savastano, "Effect of bamboo species and pre-treatment method on physical and mechanical properties of bamboo processed by flattening-densification," *Mater. Chem. Phys.*, vol. 291, no. April, p. 126746, 2022, doi: 10.1016/j.matchemphys.2022.126746.
[58] J. R. González-López, J. F. Ramos-Lara, A. Zaldivar-Cadena, L. Chávez-Guerrero, R. X. Magallanes-Rivera, and O. Burciaga-Díaz, "Small addition effect of agave biomass ashes in cement mortars," *Fuel Process. Technol.*, vol. 133, pp. 35–42, 2015, doi: 10.1016/j.fuproc.2014.12.041.
[59] Q. H. Li, Y. G. Zhang, A. H. Meng, L. Li, and G. X. Li, "Study on ash fusion temperature using original and simulated biomass ashes," *Fuel Process. Technol.*, vol. 107, pp. 107–112, 2013, doi: 10.1016/j.fuproc.2012.08.012.
[60] A. R. Pourkhorshidi, M. Najimi, T. Parhizkar, F. Jafarpour, and B. Hillemeier, "Applicability of the standard specifications of ASTM C618 for evaluation of natural pozzolans," *Cem. Concr. Compos.*, vol. 32, no. 10, pp. 794–800, 2010.
[61] I. I. Obianyo *et al.*, "Production and utilization of earth-based bricks for sustainable building applications in Nigeria: Status, benefits, challenges and way forward," *J. Build. Pathol. Rehabil.*, vol. 6, pp. 1–11, 2021.
[62] H. Haykiri-Acma, S. Yaman, and S. Kucukbayrak, "Production of biobriquettes from carbonized brown seaweed," *Fuel Process. Technol.*, vol. 106, pp. 33–40, 2013, doi: 10.1016/j.fuproc.2012.06.014.
[63] P. N. Lemougna, U. F. C. Melo, E. Kamseu, and A. B. Tchamba, "Laterite based stabilized products for sustainable building applications in tropical countries: review and prospects for the case of Cameroon," *Sustainability*, vol. 3, no. 1, pp. 293–305, 2011.
[64] E. B. Ojo, K. Mustapha, R. S. Teixeira, H. Savastano, and H. Savastano Jr, "Development of unfired earthen building materials using muscovite rich soils and

alkali activators," *Case Stud. Constr. Mater.*, vol. 11, p. e00262, 2019, doi: 10.1016/j.cscm.2019.e00262.
[65] T. T. Stanislas, A. A. Mahamat, K. Bilba, C. Onésippe-Potiron, M.-A. Arsène, and H. Savastano Jr, "Dimensional stability, durability and performance of hybrid recycled cellulose fibres reinforcing earth-based materials," *J. Compos. Mater.*, vol. 57, no. 22, pp. 3463–3478, 2023.
[66] D. Eliche-Quesada, M. A. Felipe-Sesé, J. A. López-Pérez, and A. Infantes-Molina, "Characterization and evaluation of rice husk ash and wood ash in sustainable clay matrix bricks," *Ceram. Int.*, vol. 43, no. 1, pp. 463–475, 2017, doi: 10.1016/j.ceramint.2016.09.181.
[67] A. Thennarasan Latha, B. Murugesan, and B. S. Thomas, "Compressed Stabilized Earth Block Incorporating Municipal Solid Waste Incinerator Bottom Ash as a Partial Replacement for Fine Aggregates," *Buildings*, vol. 13, no. 5, 2023, doi: 10.3390/buildings13051114.
[68] B. M. Ganou Koungang *et al.*, "Experimental thermophysical dependent mechanical analysis of earth bricks with Canarium schweinfurthii and Cocos nucifera bio-aggregates - A Case study in Cameroon," *Cogent Eng.*, vol. 10, no. 1, pp. 1–25, 2023, doi: 10.1080/23311916.2022.2159159.
[69] S. Espuelas, J. Omer, S. Marcelino, A. M. Echeverr\'\ia, and A. Seco, "Magnesium oxide as alternative binder for unfired clay bricks manufacturing," *Appl. Clay Sci.*, vol. 146, pp. 23–26, 2017.